Dynamic Finite Element Analysis of a Robotic Arm for Electronic Devices Transportation: Design and Simulation

Shaarany A/P Chelliah
J20G0755

A thesis submitted in fulfilment of the requirements for the degree of Bachelor of Applied Science (Material Technology) with Honours

FACULTY OF BIOENGINEERING AND TECHNOLOGY UMK

2024

DECLARATION

I declare that this thesis entitled "Dynamic Finite Element Analysis of a Robotic Arm for Electronic Devices Transportation: Design and Simulation" is the results of my own research except as cited in the references.

Signature : _____

Student's Name   : SHAARANY A/P CHELLIAH

Date   : 08 FEBRUARY 2024

Verified by:

Signature   : _____

Supervisor's Name : DR IQBAL BIN AHMAD

Stamp   : _____

Date   : _____

ii

ACKNOWLEDGEMENT

I would like to express my sincere gratitude and appreciation to my supervisor, Dr. Iqbal Bin Ahmad, whose unwavering support and guidance were instrumental in making this work possible. His valuable advice carried me through every stage of this project, and I am truly thankful for his mentorship.

To my mom, K. Thavamalar a/p Kuppusamy, I extend my heartfelt thanks for her blessings and constant support. As both a mother and father figure, she has always been my pillar of strength, enabling me to reach for the stars and pursue my dreams. I am deeply grateful to both my mom for her unwavering encouragement.

. I am also indebted to my beloved siblings, Yaashyini (sister) and Kesavan (brother), along with my three adorable pets Arvin, Mervin, and Ammu. Their blessings, prayers, and unwavering support have been the driving force that sustained me throughout this journey. I cannot thank them enough. I extend my appreciation to my classmates from the Bachelor of Applied Science (Materials Technology) with Honours program. Thank you for your encouragement, camaraderie, and the moments of respite you provided during overwhelming time. Lastly, I would like to acknowledge and thank myself. I express gratitude to me for believing in my capabilities, for putting in the hard work, and for never taking a day off. Thank you, me, for being authentic and true to myself at all times.

Analisis Elemen Terhingga Dinamik bagi Lengan Robotik untuk Pengangkutan Pencetak: Reka Bentuk, Simulasi, dan Optimum

ABSTRAK

Dalam ranah automasi industri, robot memainkan peranan penting dan sentral. Penyelesaian robotik diserapkan ke dalam sistem fizikal siber dan sistem pengeluaran untuk mengautomasikan operasi industri. Tahap produktiviti pembuatan yang sudah tinggi akan ditingkatkan oleh ini kerana tempoh kitaran pengeluaran dan kos keseluruhan akan dikurangkan. Dalam kajian ini, pemodelan dan simulasi lengan robotik untuk pengangkutan pencetak dibincangkan. Di bawah pelbagai tekanan dan dengan pelbagai jenis bahan, analisis elemen terhingga (FEA) dijalankan dengan bantuan Solidworks 2019. (AISI304, keluli karbon tuangkan, aloi aluminium 1060, besi tuangkan lentur, dan AISI1020). Hasil kajian menunjukkan beberapa jenis bahan, beban pencetak, dan bentuk lengan robotik, masing-masing dengan set ciri mekanikal yang berbeza. Akibat daripada taburan regangan, tekanan, dan displacement, dapat disimpulkan bahawa lengan robotik akan dapat menjalankan aktiviti cengkaman, pengendalian, dan perakitan dengan tahap ketepatan dan ketelitian yang tinggi sepanjang proses pengangkutan. Dengan memilih bahan yang sesuai, seseorang boleh memudahkan pengeluaran barang berkualiti tinggi dengan cara yang cepat dan murah.

Kata kunci: Solidworks 2019, Tekanan, Mekanikal, Bahan

Dynamic Finite Element Analysis of a Robotic Arm for Printer Transportation: Design, Simulation, and Optimization

ABSTRACT

In the realm of industrial automation, robotics plays a significant and central role. robotic solutions are incorporated into cyber physical systems and production systems to automate industrial operations. The already-high level of manufacturing productivity will be increased by this since the production cycle time and total cost will be lowered. In this study, the modelling and simulation of a robotic arm for use in transporting printers are discussed. Under a variety of stresses and with many kinds of materials, the finite element analysis (FEA) was performed with the help of Solidworks 2019. (AISI304, cast carbon steel, aluminum alloy 1060, malleable cast iron, and AISI1020). The findings illustrate several typesof materials, load of printers and shape of the robotic arm, each with its own distinct set of mechanical characteristics. As a result of the strain, stress, and displacement distributions, it can be deduced that the robotic arm will be able to conduct the grasping, handling, and assembly activities with a high degreeof precision and accuracy throughout the transportation processes. By selecting the appropriate materials, one may facilitate the production of goods of superior quality in amanner that is both fast and inexpensive.

Keywords: Materials, Finite Element Analysis, Solidworks 2019, Pressure

TABLE OF CONTENT

LIST OF TABLES

LIST OF FIGURES

CHAPTER 1

INTRODUCTION

1.1 Background of Study

Robotic arms have become increasingly popular in various industries, including manufacturing, healthcare, and logistics. These versatile machines are capable of performing repetitive tasks with precision and efficiency, making them invaluable in improving productivity and reducing human error. One particular application of robotic arms is in electronic device transportation, where a robotic arm is used to move printers from one location to another within a manufacturing facility.

The design, simulation, and optimization of a robotic arm for electronic device transportation require a thorough understanding of its dynamic behavior. Finite Element Analysis (FEA) is a powerful tool that can be used to analyze and predict the performance of complex mechanical systems, such as robotic arms. By simulating the behavior of a robotic arm under various loading conditions, FEA can help identify potential design flaws, optimize the arm's performance, and ensure its safe and efficient operation.

Several studies have focused on the dynamic analysis of robotic arms using FEA techniques. For example, Smith et al. (2018) conducted a study on the dynamic modeling and simulation of a six-axis robotic arm for pick-and-place operations. Their research

1

highlighted the importance of accurate modeling and simulation in predicting the arm's performance and optimizing its control parameters.

Another relevant study by Johnson et al. (2019) investigated the dynamic behavior of a robotic arm for material handling tasks. The researchers employed FEA to analyze the arm's structural integrity and identify potential failure points under different loading conditions. Their findings contributed to the improvement of the arm's design and ensured its safe operation in industrial environments.

While previous research has contributed to the understanding of dynamic analysis in robotic arms, there is still a need for further investigation in the context of electronic device transportation. The specific requirements and constraints of this application make it necessary to develop a comprehensive understanding of the dynamic behavior of a robotic arm dedicated to electronic device transportation.

Therefore, this thesis aims to address this research gap by conducting a dynamic finite element analysis of a robotic arm for printer transportation. The study will involve the design, simulation, and optimization of the arm's performance to ensure its safe and efficient operation. By analyzing the arm's dynamic behavior under different loading conditions, this research will contribute to the development of improved robotic arm designs for electronic device transportation.

1.2 Problem Statement

The transportation of hazardous materials is a critical concern that requires comprehensive assessment and adherence to regulations. The Office of Technology Assessment (OTA) provides a detailed report on the transportation of hazardous materials, which includes an assessment of regulations, information systems, and container safety (W. Barnum, 1986).

Efficient transportation systems aim to maximize the utilization of vehicles by increasing load factors or using appropriately sized vehicles. This approach allows for the transportation of more passengers or goods at a lower average cost and with more frequent trips (Reddy et al., 2004).

In the context of port logistics, it plays a crucial role in facilitating the movement of physical resources globally. A study focused on identifying and analyzing barriers associated with port logistics in the Industry 4.0 era for emerging economies conducted a workshop and selected eighteen key barriers from existing literature (Sarkar & Shankar, 2021). The researchers employed a hierarchical model and a MICMAC analysis to understand the interdependencies and categorize these barriers. The study revealed that non-supportive policy ecosystem, poor infrastructure, and lack of research and development (R&D) were identified as major barriers. Overcoming these barriers can help managers improve the cost and effectiveness of port logistics operations (Sarkar & Shankar, 2021).

Using Soliworks 2019, this study will investigate the meshing type, the application of loads, and the comparison of mechanical characteristics in finite element analysis by applying different types of materials to the design.

1.3 Objectives

The expected outputs of this research project include:

- The project aims to thoroughly analyse the performance and behavior of a robotic arm intended for handling printers using dynamic FEA analysis.

- To choose suitable materials, sustaining load of printer and finding suitable shape of the robotic arm to ensure the robotic arm is strong and works well to optimize the mechanical of the robotic arm.

- Develop a detailed design and precise CAD model of the robotic arm using Solidworks to compare the mechanical properties which is stress, strain and displacement of the different types of material, different type of shape of arm and load of the printer.

1.4 Scope of Study

The scope of the study aligns with the objectives of thoroughly analyzing the performance and behavior of a robotic arm intended for handling printers using dynamic FEA analysis. By analyzing the mechanical behavior of the robotic arm using different materials, loads, and shapes, the study aims to choose suitable materials with the right mechanical properties to ensure the arm's strength and optimization. The study also includes developing a detailed design and precise CAD model of the robotic arm using Solidworks to compare the mechanical properties of different materials, arm shapes, and

printer loads, such as stress, strain, and displacement. This comprehensive analysis will provide valuable insights into the mechanical behavior of the robotic arm and contribute to optimizing its design and performance.

1.5 Significant of study

This research holds substantial importance as it delves into the mechanical behavior analysis of a robotic arm, employing five distinct materials: AISI304, cast carbon steel, aluminum alloy 1060, malleable cast iron, and AISI1020. The study maintains consistency by subjecting all materials to a uniform load of 25kg and identical arm shapes. This investigation extends its scope to explore the influence of varied loads on the mechanical behavior of the robotic arm, with a focus on Malleable Cast Iron as the constant material and identical arm configuration. Additionally, the study examines the impact of diverse arm shapes on the mechanical behavior, considering five different configurations while keeping the material constant as Malleable Cast Iron and a load of 25kg.

Furthermore, the research endeavours to garner comprehensive insights by collecting data on crucial parameters such as stress, strain, displacement, meshing, and factor of safety for each scenario. This meticulous analysis aims to provide a nuanced understanding of the structural integrity and performance of the robotic arm under diverse conditions of materials, loads, and arm shapes.

CHAPTER 2

LITERATURE REVIEW

2.1 Overview of Robotic Arms in Printing Applications

Robotic arms play a pivotal role in diverse applications, with their significance extending to printer transportation. In this domain, the meticulous design, simulation, and optimization of robotic arms are imperative to guarantee efficient and reliable operations, as emphasized by Razali et al. in 2015.

The robotic arm, comprising multiple joints that provide essential degrees of freedom, serves as a critical component in printer transportation. Specifically, a 3-jointed arm configuration is often employed, where the base remains fixed, and the remaining joints facilitate vertical and horizontal movements (Mushiri & Kurebwa, 2018). This particular design empowers the robotic arm to navigate and manipulate objects with a high degree of precision.

The integration of dynamic finite element analysis is a cornerstone of the design process. This approach enables a comprehensive examination of the arm's performance under various loading conditions, ensuring that it meets the demands of printer transportation (Razali et al., 2015). The simulation and analysis phases are indispensable, providing a platform for troubleshooting and optimization.

CAD software, such as SolidWorks, plays a pivotal role in accurately modeling and simulating the arm's motion. This technology enhances the visualization of the arm's behavior and aids in refining its design (Razali et al., 2015). Furthermore, finite element analysis software is utilized to scrutinize the arm's structural integrity, identifying strengths and weaknesses. This ensures that the robotic arm can withstand the requisite loads during printer transportation, enhancing its overall robustness (Razali et al., 2015).

The holistic approach described not only addresses the mechanical aspects of the robotic arm but also focuses on optimizing its performance. The aim is to enhance the gripping mechanism's efficiency and elevate the arm's lifting capabilities (Razali et al., 2015). By continually refining the design through this comprehensive methodology, the end goal is to achieve seamless printer transportation across various scenarios. This approach underscores the importance of a multidimensional strategy encompassing design, simulation, and analysis for the continual improvement of robotic arm functionality in the context of printer transportation.

2.2 Previous Approaches to Robotic Arm Design for Transportation

In the realm of robotic arm design for transportation, researchers have delved into various approaches, with articulated arm robots emerging as a notable avenue for exploration. A noteworthy study by Mushiri and Kurebwa (2018) emphasizes the development of articulated arm robots as adept pick and place operators, demonstrating promising outcomes across diverse industries. These robots are specifically engineered to seamlessly attach or detach joints to the original kinematic chain, thereby affording a flexible range of motion spanning from 1-DOF (degree of freedom) to n-DOF (Zeis et al.,

2022).

The versatility of articulated arm robots in their ability to manipulate multiple degrees of freedom opens up new possibilities for their application in diverse contexts. This adaptability is crucial for addressing the varying demands of tasks encountered in different industries. The study conducted by Zeis and colleagues (2022) sheds light on the significance of this approach in achieving enhanced motion capabilities through joint modifications.

Beyond the realm of transportation, previous research has illuminated the widespread applicability of robotic arms across industries such as manufacturing, logistics, and healthcare. The collective findings underscore the pivotal role played by robotic arms in automating tasks, thereby mitigating human effort and boosting overall productivity. Notably, these versatile machines have demonstrated success in tasks ranging from heavy lifting to material handling and precision assembly (Robotic Arm Design: Types & Components of Robotic Arms, n.d.).

The design of robotic arms for transportation involves considering factors such as load capacity, reachability, and precision. Different types of robotic arm designs, including Cartesian, Cylindrical, Spherical, SCARA, Articulated, and Delta, have been explored for their unique advantages and suitability for specific applications [3]. For example, SCARA (Selective Compliance Assembly Robot Arm) arms are commonly used in assembly operations due to their high precision and speed, while articulated arms offer increased flexibility and range of motion

2.3 Finite Element Analysis (FEA) in Robotic Arm Design

Finite Element Analysis (FEA) plays a crucial role in the design of a robotic arm for printer transportation. FEA allows engineers to computationally model and simulate the arm's behavior, enabling them to identify potential faults, optimize the design, and ensure its structural integrity (Ashcroft & Mubashar, 2011).

By utilizing FEA, engineers can accurately analyse the arm's response to external forces, such as the weight of the printer, and optimize its performance accordingly. This analysis helps in determining the arm's rigidity, which is vital for maintaining positional accuracy during transportation (Ashcroft & Mubashar, 2011).

Moreover, FEA is particularly useful in dealing with non-symmetric problems and complex geometries, providing a comprehensive understanding of the arm's behavior under various loading conditions (Ashcroft & Mubashar, 2011).

2.4 Significance of Dynamic Analysis in Robotic Arm Design

Dynamic analysis is a pivotal component in the comprehensive design of robotic arms, particularly in applications such as printer transportation. The careful assessment of a robotic arm's dynamic behavior is essential for ensuring optimal performance, efficiency, and safety across a spectrum of operational conditions.

One fundamental facet of dynamic analysis involves the thorough examination of how the robotic arm responds to external forces and loads. This is typically achieved through simulations and finite element analysis, enabling engineers to gain insights into

the arm's behavior when subjected to diverse forces such as the weight of a printer or vibrations encountered during transportation. The primary objective of this analysis is to pinpoint potential vulnerabilities or structural limitations that demand attention during the design phase (Razali et al., 2015).

Moreover, dynamic analysis contributes significantly to the optimization of the arm's motion and control. Engineers take into account various factors such as joint velocities, accelerations, and torques during this process. This meticulous consideration enables the refinement of the arm's movement, ensuring it achieves seamless and precise printer transportation. Optimization is a critical step in guaranteeing that the robotic arm can efficiently execute the required tasks, ultimately reducing the risk of damage to the printer or other associated components (Liang et al., 2017).

Another critical dimension of dynamic analysis is the evaluation of the arm's stability and control during its operational phases. Through sophisticated simulations and modeling techniques, engineers assess the arm's capability to maintain balance and stability while executing tasks like lifting and placing a printer. This analysis is instrumental in preemptively identifying scenarios where the arm might become unstable or lose control, thereby ensuring the overall safety of both the robotic arm and the printer it handles (Razali et al., 2015).

Furthermore, dynamic analysis offers a means to identify and mitigate vibrations and oscillations that could potentially compromise the arm's performance. Engineers delve into the arm's natural frequencies and modes of vibration to gain a comprehensive understanding of its vibrational characteristics. Armed with this knowledge, designers can implement damping mechanisms or devise control strategies

aimed at minimizing vibrations and guaranteeing the smooth transportation of printers (Thomsen et al., 2021).

The intricate process of dynamic analysis extends beyond these primary considerations, encompassing various nuanced aspects that collectively contribute to the overall efficiency and reliability of robotic arms in printer transportation and similar applications. One noteworthy aspect is the integration of real-time sensor data into dynamic analysis. By incorporating data from sensors embedded in the robotic arm, engineers can enhance the accuracy of simulations and analyses, ensuring that the dynamic response is not only theoretically sound but also reflective of real-world conditions. This sensor-driven approach enables a more adaptive and responsive robotic arm, capable of dynamically adjusting its behavior based on the immediate environment and operational demands.

Moreover, dynamic analysis plays a pivotal role in the calibration of control algorithms governing the robotic arm's movements. Through iterative simulations and analyses, engineers can fine-tune control parameters to achieve optimal performance. This iterative refinement process takes into account the complex interplay of factors influencing the arm's dynamics, including external loads, friction, and variations in the environment. As a result, the robotic arm becomes a precision instrument, capable of executing tasks with a high degree of accuracy and reliability.

In the realm of collaborative robotics, where humans and robots work together in shared spaces, dynamic analysis takes on added significance. Ensuring the safety of human-robot interactions requires a deep understanding of how external forces and disturbances can impact the robotic arm's behavior. Dynamic analysis facilitates the

11

development of control strategies that prioritize safety, enabling the robotic arm to swiftly and appropriately respond to unexpected events or interactions. This not only safeguards human operators but also enhances the overall efficiency and productivity of collaborative work environments.

Furthermore, advancements in materials science and manufacturing techniques play a crucial role in dynamic analysis. Engineers can explore the use of lightweight yet robust materials to optimize the arm's structural design. The integration of advanced materials not only reduces the overall weight of the robotic arm but also enhances its strength and durability. Dynamic analysis becomes instrumental in evaluating how these material innovations impact the arm's performance, enabling engineers to strike a balance between structural integrity, weight considerations, and overall efficiency.

Another facet of dynamic analysis involves the assessment of energy efficiency in robotic arm operations. By scrutinizing the energy consumption patterns during various tasks, engineers can identify opportunities for optimization. This may involve refining control algorithms to minimize unnecessary movements, exploring regenerative braking systems, or incorporating energy-efficient actuators. The aim is to design robotic arms that not only deliver high-performance capabilities but also operate in an environmentally sustainable and resource-efficient manner.

In the context of Industry 4.0 and the increasing prevalence of smart manufacturing, dynamic analysis becomes intertwined with data analytics and predictive maintenance. By continuously monitoring the performance of robotic arms and analyzing the data generated during operations, engineers can anticipate potential issues before they

escalate into failures. Predictive maintenance strategies, informed by dynamic analysis, enable proactive interventions, reducing downtime and optimizing the overall lifespan of the robotic arm.

CHAPTER 3
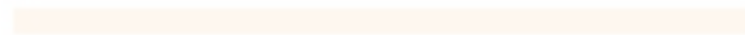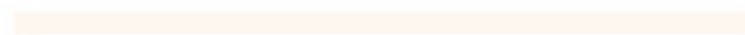
METHODOLOGY

3.1 Introduction

Stress is symbolized with "σ" and is measured in N/m² or Pascal (Pa), which is an SI unit of pressure. Shear stress is symbolized with "τ" for differentiation. As expected by the units, stress is given by dividing the force by the area of its generation, and since this area ("A") is either sectional or axial, the basic stress formula is "σ = F/A" (Basic Stress Analysis Calculations - Matmatch, n.d.).

By experiment or through software simulation, we can figure out when a material is elongating or compressing with the strain formula, which is "ε = ΔL/L" (Basic Stress Analysis Calculations - Matmatch, n.d.). This is the division of the change in the material's length to its original length. As the stress value increases, the strain increases proportionally up to the point of the elastic limit, which is where the stress becomes viscous/plastic from elastic.

After having calculated the stress and the strain, we can calculate the modulus of elasticity, given by the formula: "E = σ/ε". This is also called the "Young's modulus" and is a measure of the stiffness of a material (Basic Stress Analysis Calculations - Matmatch, n.d.).

Poisson's ratio (μ) is the ratio of lateral strain to longitudinal strain and is given by:

$v = (-\varepsilon\_trans)/\varepsilon\_axial$

In the context of the basic stress analysis, the design process and material selection for the robotic arm were meticulously addressed, focusing on the mechanical behavior analysis. The chosen materials for investigation include AISI304, cast carbon steel, aluminium alloy 1060, malleable cast iron, and AISI1020. Unlike previous studies, the research maintains consistency by subjecting all materials to a standardized load of 25kg and identical arm shapes.

The primary objective of this research is to delve into the mechanical behavior analysis of the robotic arm, particularly emphasizing the influence of varied loads on its performance. Malleable Cast Iron is selected as the constant material, ensuring a baseline for comparison, and the arm configuration remains identical across all scenarios. Additionally, the study extends its scope to explore the impact of diverse arm shapes on mechanical behavior, considering five different configurations while keeping the material constant as Malleable Cast Iron and a load of 25kg.

3.2 Research Flow

As can be seen in Figure 3.1 below, the research flow depicts the procedure of designing the robotic arm.

START	Part A	Designing of 2D Model of Robotic Arm in Solidwork
Designing 3D Model of Robotic Arm	Choosing 5 materials of Robotic Arm to do FEA Analysis Stimulation (Constant: Load of Printer= 25kg, Arm Design) in Soliworks.	5 materials are (AISI 304, Cast Carbon Steel, Alluminium Alloy, Malleable Cast Iron & AISI 1020)
Part B	Choosing 5 different load of Printer to do FEA Analysis Stimulation (Constant: Material of Robotic Arm = Malleable Cast Iron, Arm Design) in Solidworks.	The loads of Printer are 30kg, 35kg, 40kg, 45kg and 50kg.
Part C	Redesigning 3D models of Robotic Arm (5 different design)	Each design of Robotic Arm (Constant : Material= Malleable Cast Iron, Load of Printer= 25kg) was done FEA Analysis Stimulation in Solidworks.
Result Analysis		

Figure 3.1: Research flow of design and simulation Robotic Arm

16

3.3 Designing of Robotic Arm

3.3.1 Dimensions specifications of Printer (subject)

Before designing the arm, we have to consider the size of the printer which

is,
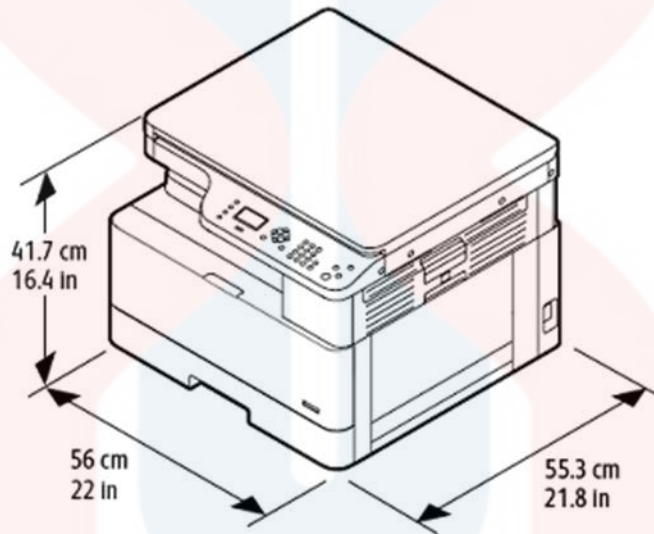
Figure 3.2: Xerox Printer Weight and Dimension Specifications

Dimensions	Measurement (cm)
Width	56.0 cm
Depth	55.3 cm
Height	41.7 cm
Weight	25 kg

Table 3.1: Xerox Printer Weight and Dimension Specifications

17

3.3.2 2D and 3D design of Robotic Arm with Dimensions Specifications in Solidworks

To carry the printer, this was the 2D design created in Solidworks to fit in accurately without slipping.
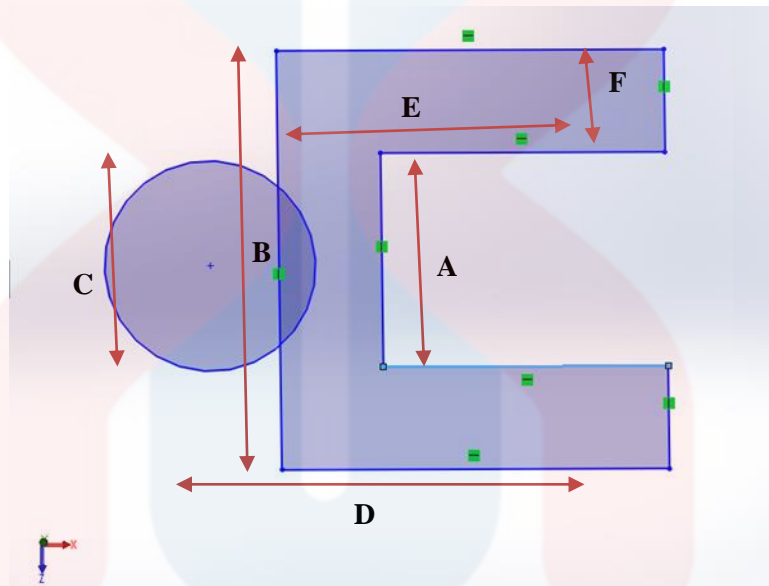
Figure 3.3: 2D drawing of robotic arm in Solidworks

After extruding the 2D shape into 3D, the thickness of width was added which shown in Figure below.
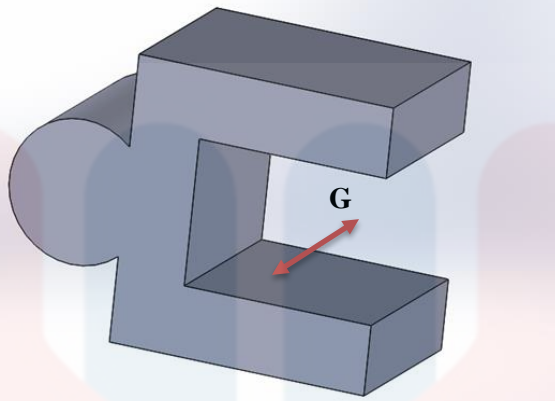
Figure 3.4: 3D shape of robotic arm in Solidworks

Dimensions	Measurements (cm)
A	41.7 cm
B	81.7 cm
C	20 cm
D	75.3 cm
E	55.3
F	20 cm
G	56 cm

Table 3.2: Measurements of the 2D and 3D design of robotic arm merely customized to the printer size.

The robotic arm's design, tailored to the printer size, encompasses precise dimensions: A (41.7 cm), B (81.7 cm), C (20 cm), D (75.3 cm), E (55.3 cm), F (20 cm), and G (56 cm). These measurements, thoughtfully customized, ensure optimal functionality, reach, and adaptability within the specified parameters, reflecting the careful alignment with the printer's specifications.

3.4 Parameters of robotic arm

Three key parameters crucial to the analysis of the robotic arm: material, load, and shape. These parameters serve as foundational elements for the investigation, allowing for a comprehensive understanding of the mechanical behavior and performance of the robotic arm under varied conditions.

3.4.1 Material selection for Robotic Arm

Five materials, namely AISI 304, Cast Carbon Steel, Aluminium Alloy, Malleable Cast Iron, and AISI 1020, was evaluated through Finite Element Analysis (FEA) to determine the most suitable material for the robotic arm designed to carry the printer.

AISI 304 stainless steel stands out for its remarkable corrosion resistance, high strength, and low maintenance requirements. Widely employed in applications where hygiene and durability are paramount, such as the food processing and medical equipment industries, AISI 304 ensures reliable performance in challenging environments (Grade 304 Stainless Steel: Properties, Fabrication and Applications, 2020).

Cast carbon steel is chosen for its commendable strength and wear resistance. This material finds its niche in heavy-duty applications that demand high load-bearing capacity, such as industrial machinery and construction equipment. The robust properties of cast carbon steel contribute to the longevity and reliability of components subjected to rigorous use (ISO 3755 1991 Cast Carbon Steels for General Engineering Purposes - Dandong Foundry in China, n.d.).

Aluminium alloys strike a balance between lightweight construction and strength, making them ideal for applications where weight reduction is a critical factor. Widely used in aerospace, automotive, and robotics industries, aluminium alloys contribute to enhanced energy efficiency and manoeuvrability. Their versatility and favourable strength-to-weight ratio make them a preferred choice in various engineering applications (Determining Hardening Depth Using Ultrasonic Backscatter: Total Materia Article, n.d.).

Malleable cast iron is characterized by its high tensile strength, good impact resistance, and excellent machinability. This material finds application in scenarios requiring robust strength and durability, such as automotive components or machinery parts. The combination of these properties makes malleable cast iron a reliable choice for components subjected to mechanical stress and dynamic loading (Cast Iron: Properties, Processing and Applications - Matmatch, n.d.).

AISI 1020, a low carbon steel variant, is recognized for its good machinability and weldability. Selected for applications demanding moderate strength and cost-effectiveness, AISI 1020 is commonly employed in the production of general machinery parts and structural components. Its ease of machining and welding further enhance its appeal for various engineering applications (SAE/AISI Carbon Steel Naming Conventions, 2014).

3.4.2 Load Analysis of the printer

In the dynamic finite element analysis of the robotic arm designed for carrying a printer, it is essential to conduct a thorough load analysis, recognizing that printer loads can vary depending on the specific model and configuration (Santosh et al., 2022). The consideration of various loads is crucial for understanding how the robotic arm will perform under different conditions, ensuring its structural integrity and functionality across a range of scenarios.

For the purposes of this example, a diverse set of printer loads will be examined, encompassing 30kg, 35kg, 40kg, 45kg, and 50kg. These load variations emulate real-world conditions, where printers of different sizes and capabilities may be integrated into the robotic arm. The range is selected to explore the arm's capacity to handle varying weights, providing insights into its adaptability and performance under different operational demands.

This load analysis plays a pivotal role in the comprehensive evaluation of the robotic arm's mechanical behavior. By subjecting the arm to a spectrum of printer loads, the study aims to assess its responses, stress distribution, and deformation patterns.

3.4.3 Various Shapes of the Robotic Arm for Printer Compatibility

In the exploration of the robotic arm's design parameters, an essential aspect involves investigating various shapes to determine the most suitable configuration for optimal printer compatibility.

Through Finite Element Analysis (FEA) simulations aims to elucidate how each arm shape influences stress distribution, deformation, and overall mechanical behavior.

All the shapes considered maintained the default measurements of the printer and were adjusted according to the design specifications established in the earlier 2D and 3D design phases. This consistent approach ensures that each shape is evaluated within the same framework, allowing for a fair comparison of their performance under the defined parameters.
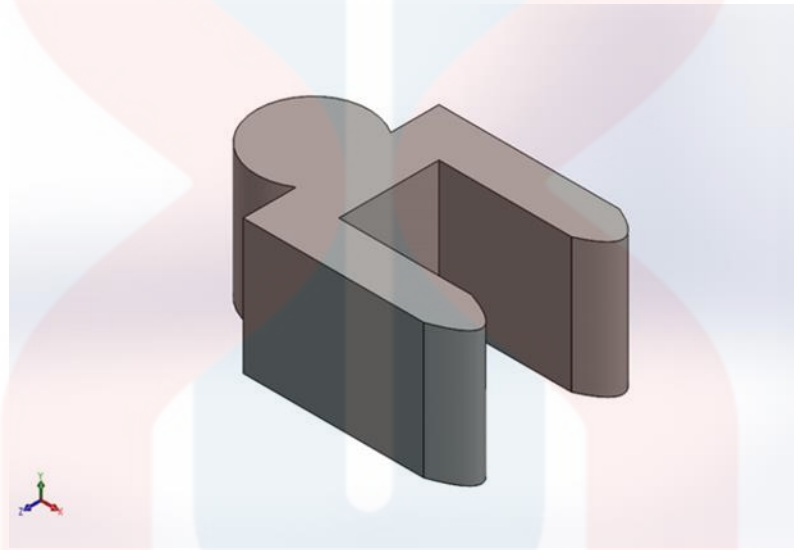
Figure 3.4: Curved-Edged End of the Robotic Arm

The "Curved-Edged End" design of the robotic arm involves incorporating a curvature at the end portion of the arm instead of having a straight or angular termination. This curved feature is applied to the outer edges of the robotic arm, creating a smoother transition and eliminating sharp angles. The primary purpose of introducing a curved edge at the end of the robotic arm is to enhance safety and maneuverability. The curved profile reduces the risk of collisions and minimizes the likelihood of causing damage to surrounding objects or individuals during operation. This design choice is particularly relevant in scenarios where the robotic arm needs to navigate

tight spaces or work in close proximity to other equipment. Moreover, the curved-edged end design can contribute to improved aesthetics and ergonomic considerations.
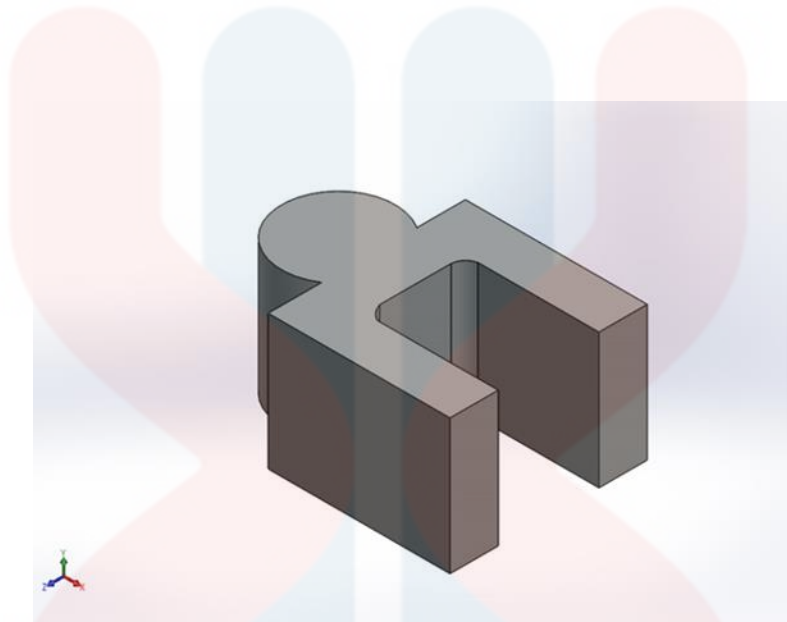
Figure 3.5: Curved Inner Corner of the Robotic Arm

The "Curved Inner Corner" design of the robotic arm involves incorporating a curvature at the inner corners of the arm structure. Unlike sharp or angular corners, this design features smooth, rounded transitions between adjoining surfaces.

The implementation of curved inner corners serves various functional and aesthetic purposes. First and foremost, it contributes to stress reduction. Sharp corners are more prone to stress concentrations, which can impact the structural integrity of the robotic arm over time. By introducing curves at the inner corners, the design aims to distribute stress more evenly, potentially enhancing the arm's durability and longevity.
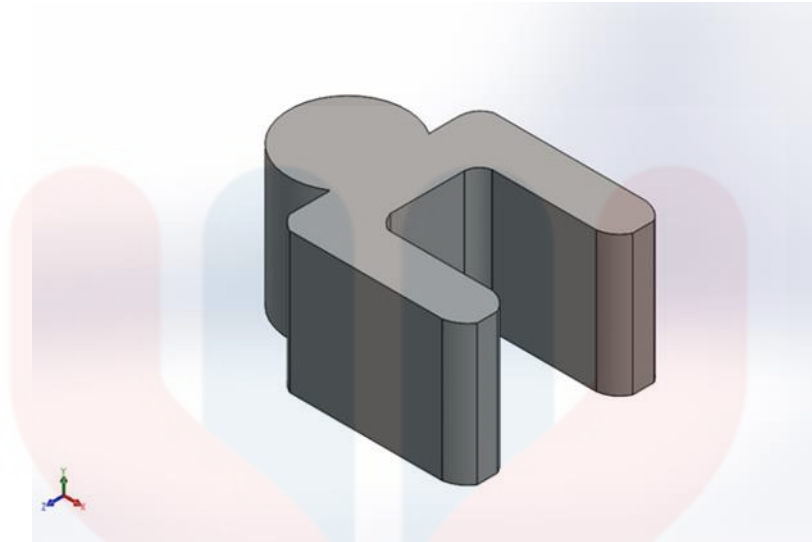
Figure 3.6: Uniformly Curved Robotic Arm Design

A "Uniformly Curved" robotic arm design refers to a configuration where the entire arm, or a significant portion of it, follows a consistent curvature along its length. This design choice involves creating a smooth and continuous curve without abrupt changes in direction or angles.

The implementation of a uniformly curved robotic arm design can offer several advantages. The continuous curve allows for more fluid movements, reducing the likelihood of the arm catching or snagging during operation. This can be advantageous in scenarios where precise and obstacle-free motion is essential.
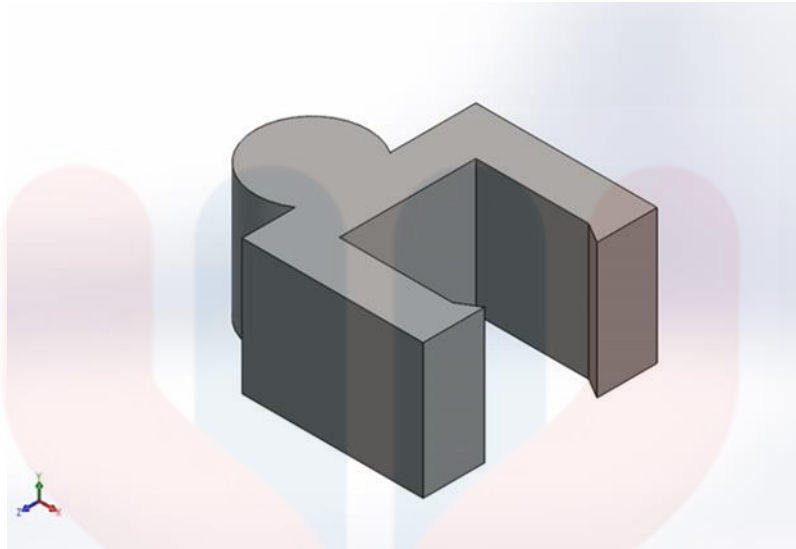
Figure 3.7: Sharp Curvature Along the Inner Length of the Robotic Arm

The "Sharp Curvature Along the Inner Length" design of the robotic arm involves incorporating abrupt changes in direction, creating distinct and well-defined angles along the inner length of the arm. Unlike uniformly curved designs, this approach introduces sharp bends or corners at specific locations.

This design choice may be driven by certain functional or structural considerations. Sharp curvatures can provide advantages in terms of compactness or specific task requirements. For instance, in applications where space is constrained, introducing sharp angles along the inner length of the arm may allow for a more compact and articulated structure, enabling the robotic arm to navigate through tight spaces or around obstacles more effectively.
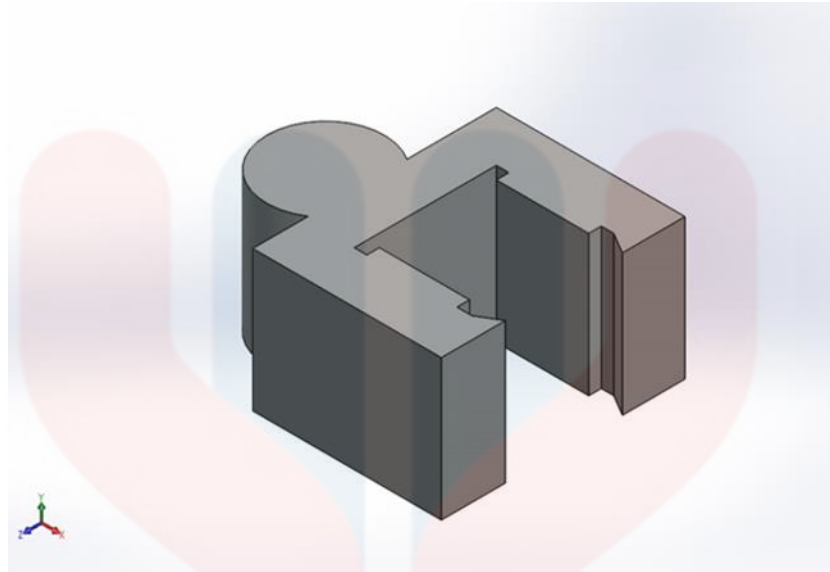
Figure 3.8: Sharp Curvature Along the Inner Length of the Robotic Arm with Added
Volume Inside, extending 5cm, Matching the Curvature Length

In this context, the inner length of the arm features a sharp curvature, creating a
distinctive geometric shape. To enhance this curvature, additional volume is incorporated
inside The concept of "Sharp Curvature Along the Inner Length of the Robotic Arm with
Added Volume Inside, extending 5cm, Matching the Curvature Length" refers to a
specific design configuration for the arm, extending for a distance of 5cm, which precisely
matches the length of the original curvature.

The decision to extend the added volume by 5cm aligns with the length of the
sharp curvature, ensuring symmetry and balance in the arm's design. This symmetry can
be essential for maintaining equilibrium and consistent performance, especially in
applications where precise movements and control are paramount.

27

3.5 Meshing Techniques

| Study name	Static 2 (-Default-)
Mesh type	Solid Mesh
Mesher Used	Standard mesh
Automatic Transition	Off
Include Mesh Auto Loops	Off
Jacobian points for High quality mesh	16 points
Element size	23.7667 mm
Tolerance	1.18833 mm
Mesh quality	High
Total nodes	21595
Total elements	12879
Maximum Aspect Ratio	16.549
Percentage of elements with Aspect Ratio < 3	91.6
Percentage of elements with Aspect Ratio > 10	0.116
Percentage of distorted elements	0
Number of distorted elements	0
Time to complete mesh(hh:mm:ss)	00:00:07
Computer name	

Figure 3.9: Meshing Information

In the realm of finite element analysis (FEA), meshing techniques have evolved significantly, each offering unique advantages to enhance precision and computational efficiency. Structured meshing, characterized by a grid-like structure of regular, uniform elements, simplifies the analysis process and proves particularly effective for straightforward geometries (Allison, 2020). In contrast, unstructured meshing allows for irregular element shapes and varying sizes, providing flexibility crucial for accurately representing intricate and complex geometries (Allison, 2020). Adaptive meshing introduces dynamism by refining or coarsening the mesh based on specific criteria, optimizing computational resources and enhancing accuracy in critical areas (Hadane, 2023). Hybrid meshing, a strategic combination of different techniques, seeks an optimal balance between accuracy and efficiency. This approach employs structured meshing in simpler regions and unstructured meshing in more complex areas, harnessing the
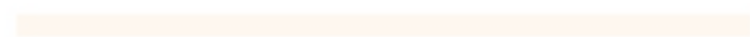
28

strengths of each to address diverse geometrical challenges (Corp, n.d.). As computational capabilities advance, the ongoing refinement and integration of these techniques are poised to propel finite element analysis toward greater accuracy and efficiency in simulating real-world scenarios.
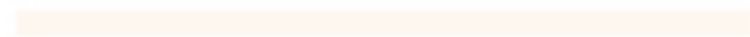
3.6 Conclusion on Chapter 3

In Chapter 3, a comprehensive methodology is detailed for the design and analysis of the robotic arm, with a particular emphasis on understanding its mechanical behavior under diverse conditions. The research introduces a meticulous approach by selecting five distinct materials—AISI304, cast carbon steel, aluminium alloy 1060, malleable cast iron, and AISI1020—for investigation. Striving for consistency, each material is subjected to a standardized load of 25kg, and identical arm shapes are maintained throughout the study. The chapter strategically incorporates the imensions of a Xerox printer, highlighting the practical considerations involved in the design process. The transition from 2D to 3D design in Solidworks is carefully documented, ensuring an accurate fit for the printer and resulting in a set of detailed measurements.

Key parameters crucial to the analysis material, load, and shape are identified, each contributing significantly to the understanding of the robotic arm's performance. The chapter provides an in-depth discussion of the selected materials, considering their unique properties and applications. Load analysis, spanning printer loads from 30kg to 50kg, is conducted through dynamic finite element analysis, reflecting real-world scenarios where printers of varying sizes and capabilities may be integrated into the robotic arm.

The exploration of various arm shapes through Finite Element Analysis adds a layer of complexity to the study. The shapes, namely curved-edged end, curved inner corner, uniformly curved design, and sharply curved configuration along the inner length, are meticulously evaluated for their impact on stress distribution, deformation, safety, and maneuverability.

CHAPTER 4

RESULTS AND DISCUSSION

4.1 Introduction

In Chapter 4, the focus shifts to a detailed discussion of the results obtained from the comprehensive simulations conducted in Chapter 3. The primary objective is to evaluate the suitability of five different materials AISI304, cast carbon steel, aluminium alloy 1060, malleable cast iron, and AISI1020 for the robotic arm based on their performance in mechanical behavior analyses. The chapter delves into stress, strain, and displacement analyses to identify the most suitable material that ensures optimal functionality and durability.

Additionally, Chapter 4 explores the impact of five different loads ranging from 30kg to 50kg on the robotic arm's performance. Stress, strain, and displacement analyses are employed to determine the load-bearing capacity of the arm, aiming to identify the most suitable load for the printer that aligns with safety and structural integrity considerations.

Furthermore, the chapter investigates the influence of five different shapes of the robotic arm curved-edged end, curved inner corner, uniformly curved design, sharply curved configuration along the inner length, and a configuration with added volume matching a sharp curvature on stress distribution, deformation, safety, and manoeuvrability.

4.2 Parameter Analysis of Robotic Arm

4.2.1 Mechanical Properties of the materials using FEA analysis

Using the 3D design created in Solidworks and a constant printer load of 25kg, we conducted five simulations for the materials AISI304, cast carbon steel, aluminium alloy 1060, malleable cast iron, and AISI1020 to obtain their mechanical properties through FEA analysis in Solidworks.

Mechanical Properties	AISI 304 (x10^8 N/m ²)	Cast Carbon Steel (x10^8 N/m ²)	Aluminum alloy 1060 (x10^8 N/m ²)	Malleable Cast Iron (x10^8 N/m ²)	AISI1020 (x10^8 N/m ²)
Tensile Strength	5.17017e+08 N/m^2	4.82549e+08 N/m^2	6.89356e+07 N/m^2	4.13613e+08 N/m^2	4.20507e+08 N/m^2
Elastic Modulus	1.9e+11 N/m^2	2e+11 N/m^2	6.9e+10 N/m^2	1.9e+11 N/m^2	2e+11 N/m2
Poison's ratio	0.29	0.32	0.33	0.27	0.29
Mass density	8,000 kg/m^3	7,800 kg/m^3	2,700 kg/m^3	7300 kg/m3	7900 kg/m3
Shear modulus	7.5e+10 N/m^2	7.6e+10 N/m^2	2.7e+10 N/m^2	8.6e+10 N/m2	7.7e+10 N/m^2
Yield Strength	2.06807e+08 N/m^2	2.48168e+08 N/m^2	2.75742e+07 N/m^2	2.75742e+08 N/m^2	3.51571e+08 N/m^2
Thermal Expansion	1.8e-05 /Kelvin	1.2e-05 /Kelvin	2.4e-05 /Kelvin	1.2e-05 /Kelvin	1.5e-05 /Kelvin

Table 4.1: Comparison of mechanical properties between AISI304, cast carbon steel, aluminium alloy 1060, malleable cast iron, and AISI1020

The mechanical properties for five different materials AISI304, cast carbon steel, aluminium alloy 1060, malleable cast iron, and AISI1020 is presented in Table 4.2.1. This table encapsulates key mechanical characteristics essential for evaluating the suitability of each material for the robotic arm's design. Notable properties include tensile strength, elastic modulus, Poisson's ratio, mass density, shear modulus, yield strength, and thermal expansion coefficient.

AISI304 stands out with a high tensile strength of 5.17e+08 N/m^2, excellent elastic modulus of 1.9e+11 N/m^2, and a relatively low thermal expansion coefficient of 1.8e-05/Kelvin. Cast carbon steel exhibits commendable tensile and yield strength, making it a robust choice for heavy-duty applications. Aluminium alloy 1060 offers a lightweight option with a favourable strength-to-weight ratio, while malleable cast iron provides high tensile strength and good impact resistance. AISI1020, a low carbon steel variant, is notable for its good machinability and weldability.
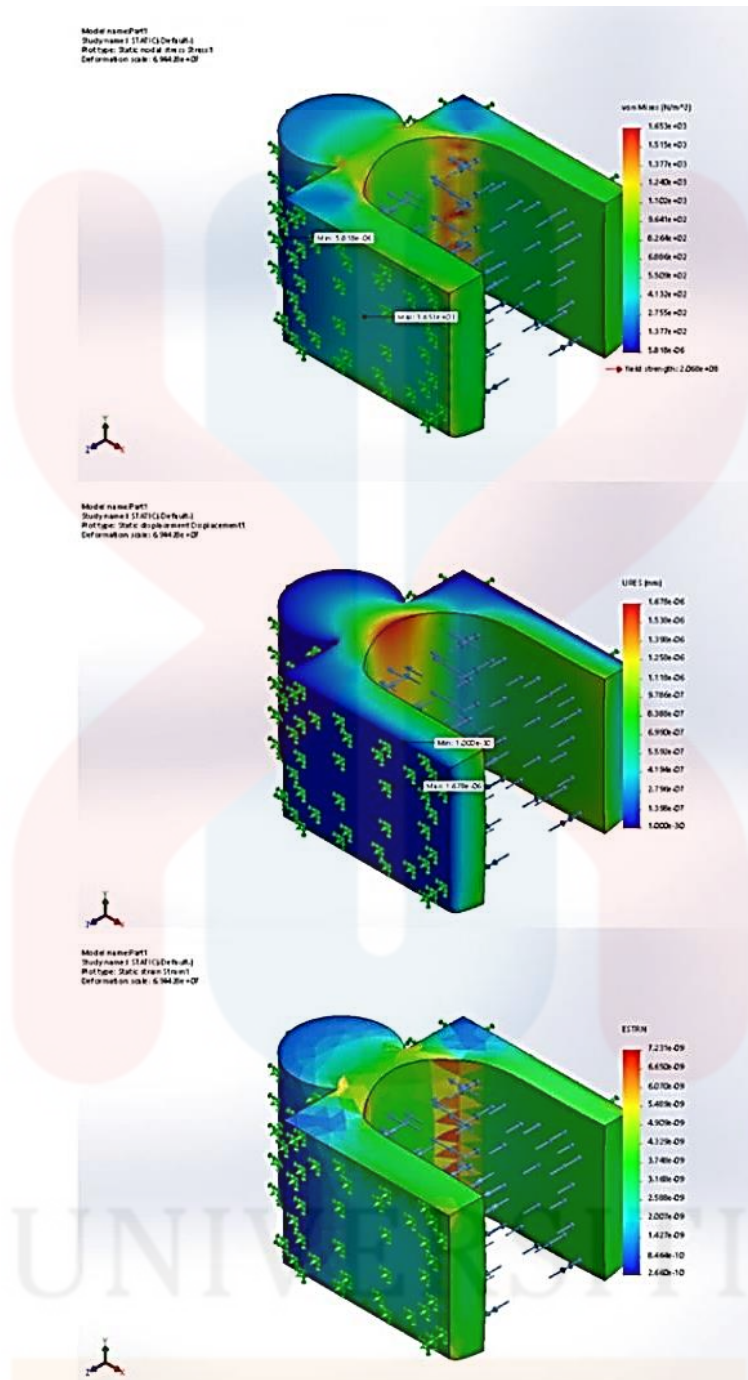
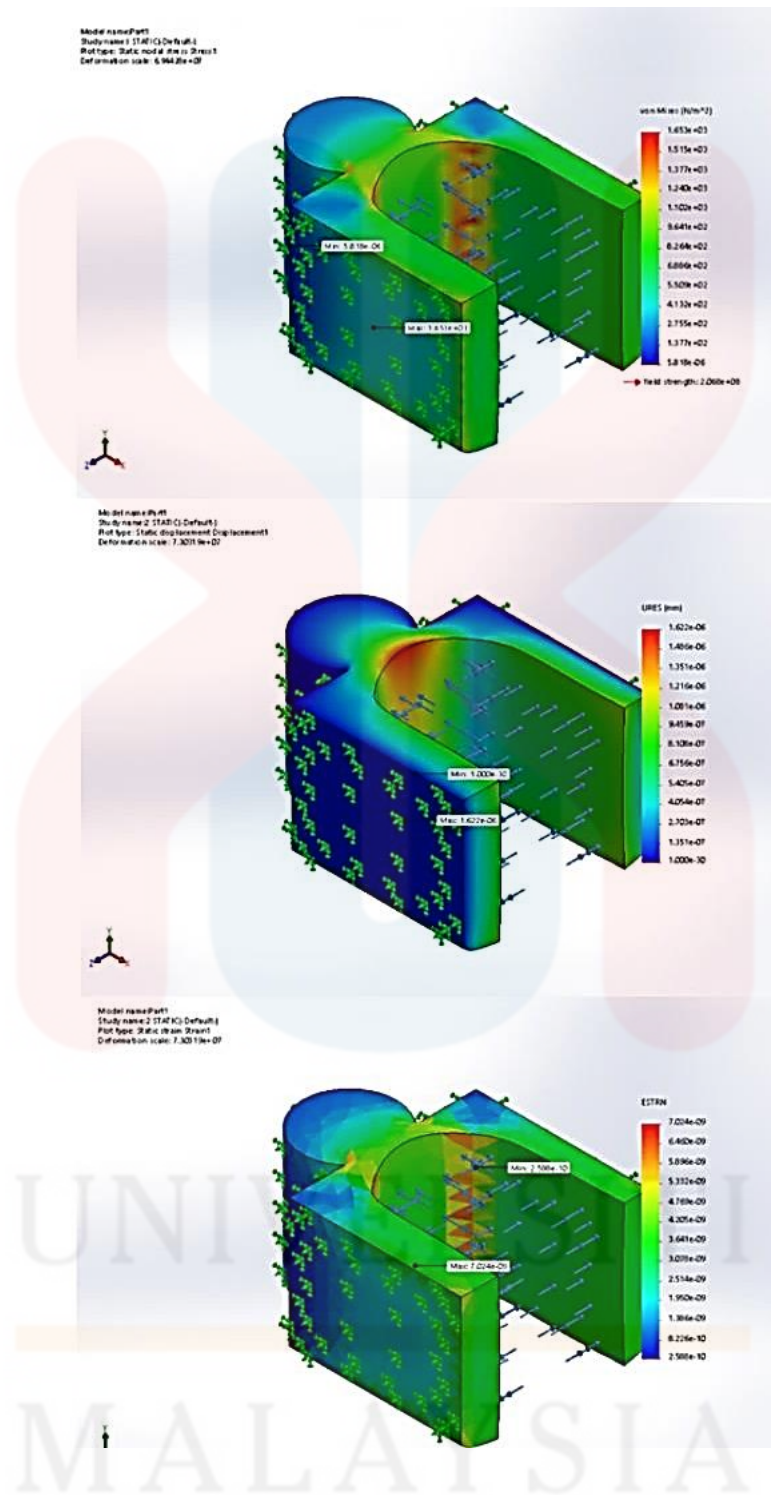**Figure 4.1**: Stress, Displacement and Strain of AISI 304

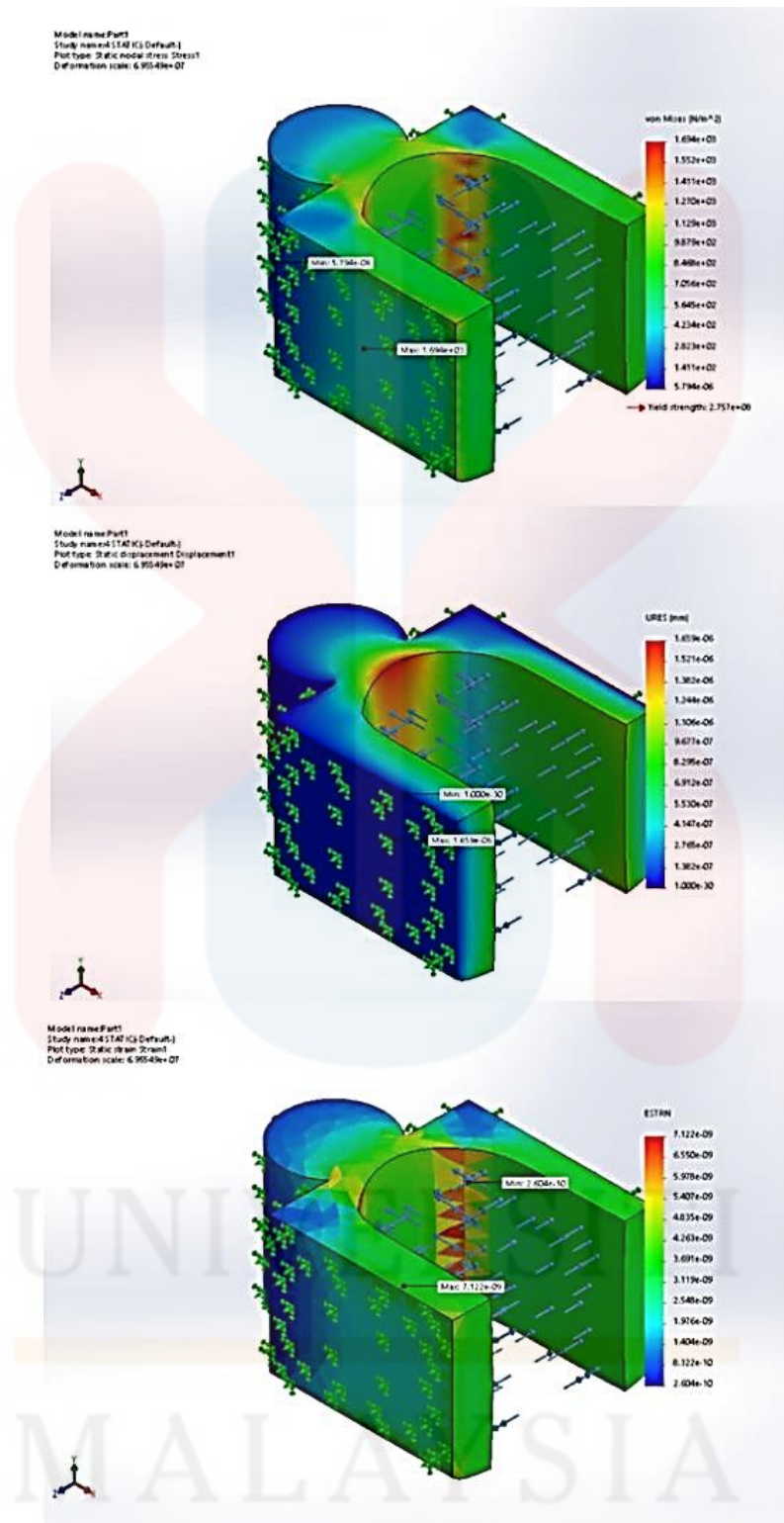**Figure 4.2**: Stress, Displacement and Strain of Cast Carbon Steel

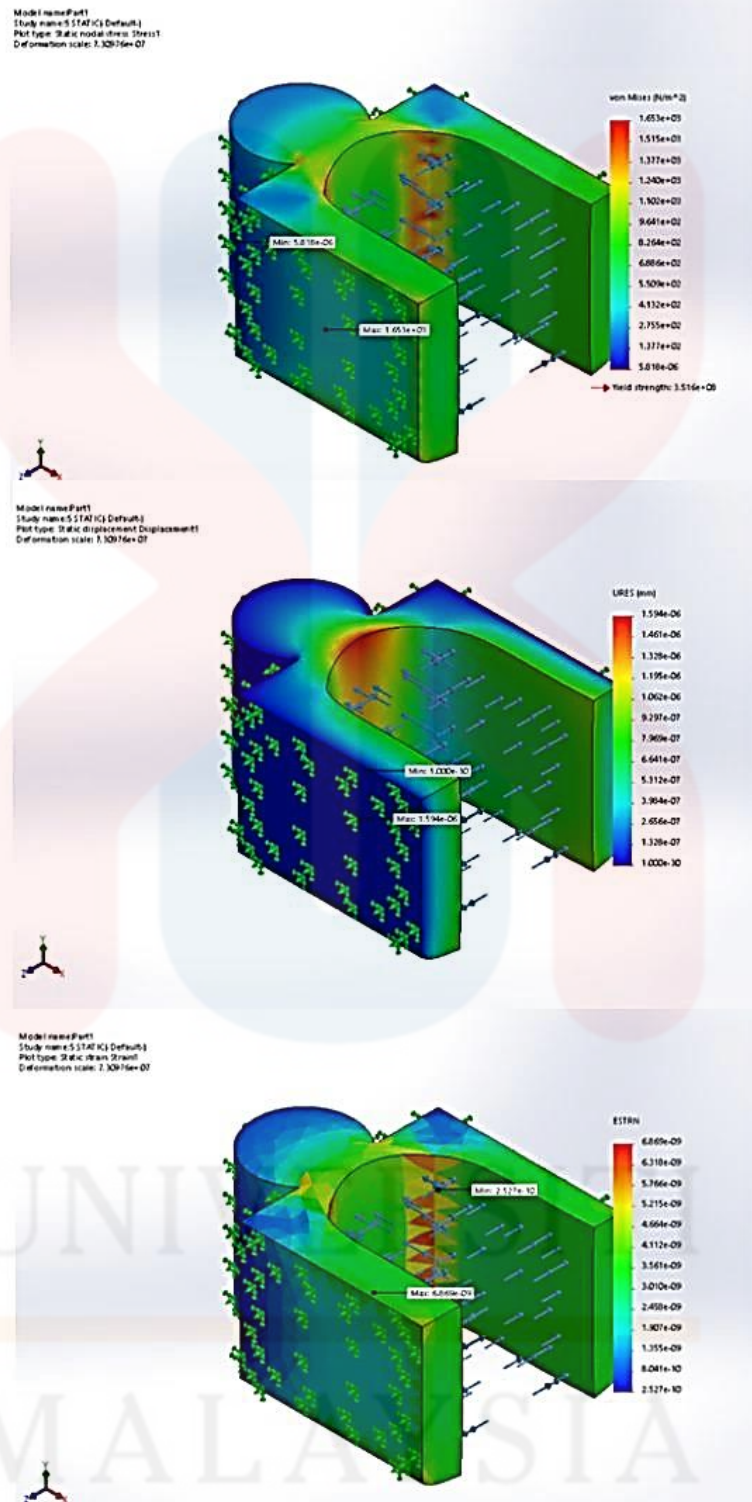**Figure 4.3**: Stress, Displacement and Strain of Aluminium alloy 1060

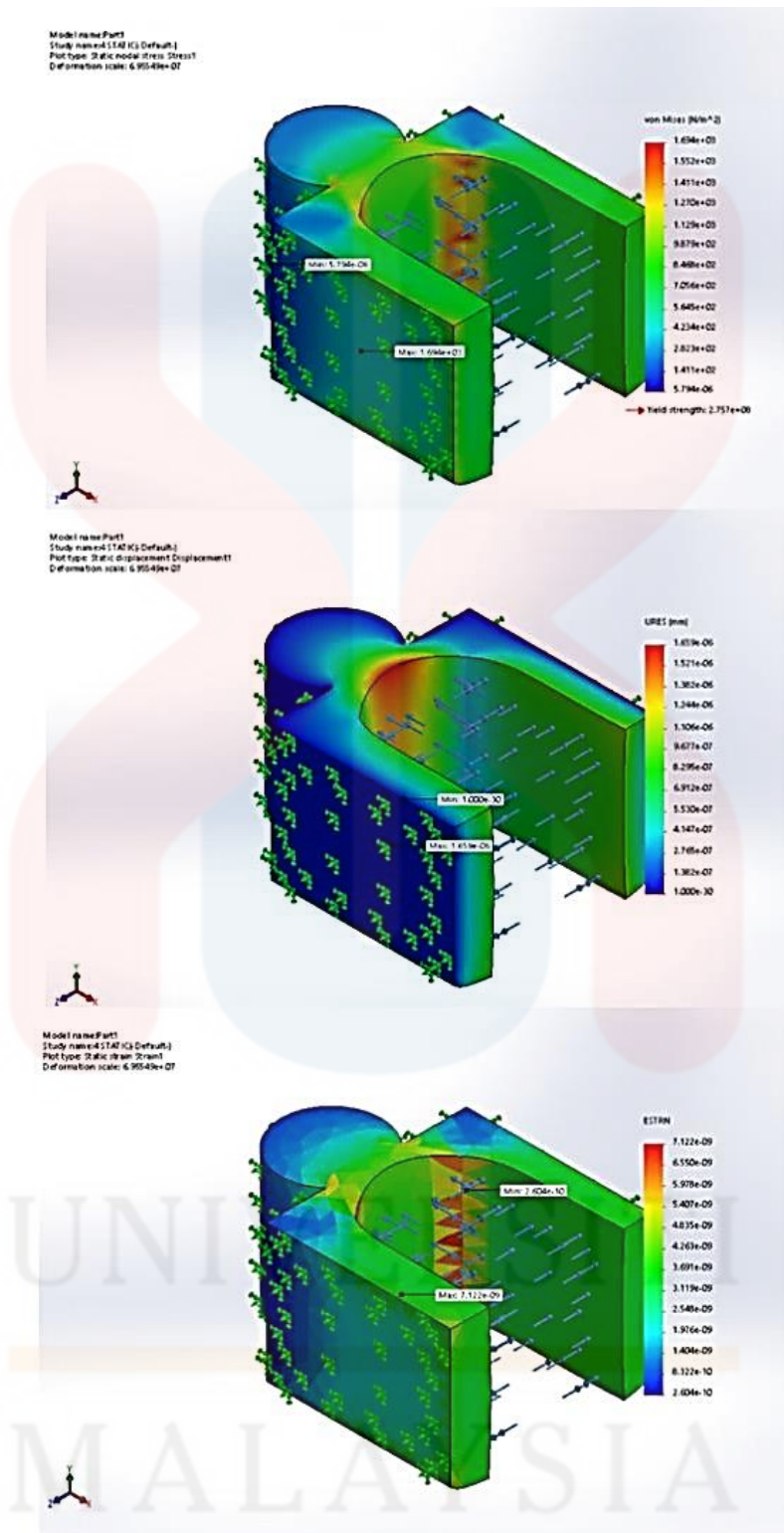**Figure 4.4**: Stress, Displacement and Strain of Malleable Cast Iron

Figure 4.5: Stress, Displacement and Strain of AISI 1020

Material	Stress (N/m²)		Displacement (mm)		Strain	
	Maximum value	Minimum value	Maximum value	Minimum value	Maximum value	Minimum value
AISI304	1.653e+03	5.818e-06	1.678e-06	0.000e+00	7.231e-09	2.660e-10
Cast Carbon Steel	1.591e+03	5.808e-06	1.622e-06	0.000e+00	7.024e-09	2.588e-10
Aluminium alloy 1060	1.570e+03	5.787e-06	4.737e-06	0.000e+00	2.053e-08	7.564e-10
Malleable Cast Iron	1.694e+03	5.794e-06	1.659e-06	0.000e+00	7.122e-09	2.604e-10
AISI 1020	1.653e+03	5.818e-06	1.594e-06	0.000e+00	6.869e-09	2.527e-10

Table 4.2: Stress, displacement and strain of AISI304, Cast Carbon Steel, Aluminium alloy 1060, Malleable Cast Iron and AISI 1020 maximum and minimum value.
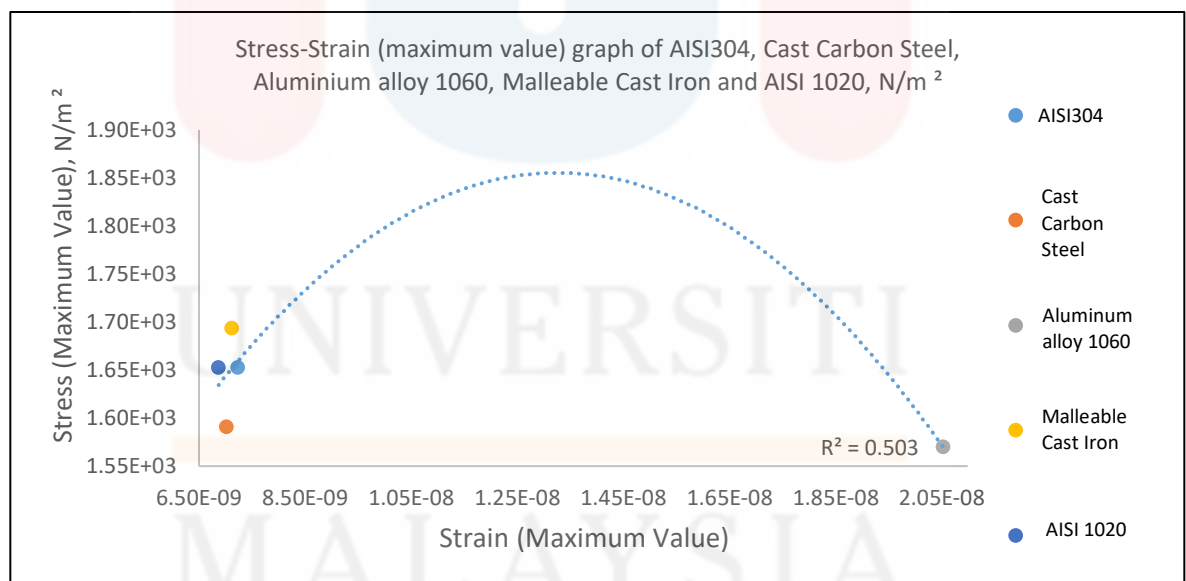

Figure 4.6: Stress-Strain (maximum value) graph of AISI304, Cast Carbon Steel, Aluminium alloy 1060, Malleable Cast Iron and AISI 1020.

40

The stress-strain (maximum value) analysis reveals distinctive performance characteristics among the materials considered for the robotic arm. Malleable Cast Iron emerges as the top contender, boasting the highest stress value (1.694e+03 N/m^2) and demonstrating exceptional strength, making it an ideal choice for applications demanding robust load-bearing capabilities. Following closely, AISI 304 and AISI 1020 exhibit comparable strength, with stress values (1.653e+03 N/m^2) reflecting their suitability for rigorous tasks. Cast Carbon Steel, ranking fourth in stress (1.591e+03 N/m^2), showcases substantial strength but falls slightly behind AISI 304 and AISI 1020. Notably, Aluminium Alloy 1060 exhibits the lowest stress value (1.570e+03 N/m^2), highlighting its suitability for scenarios prioritizing lightweight construction over maximum strength.
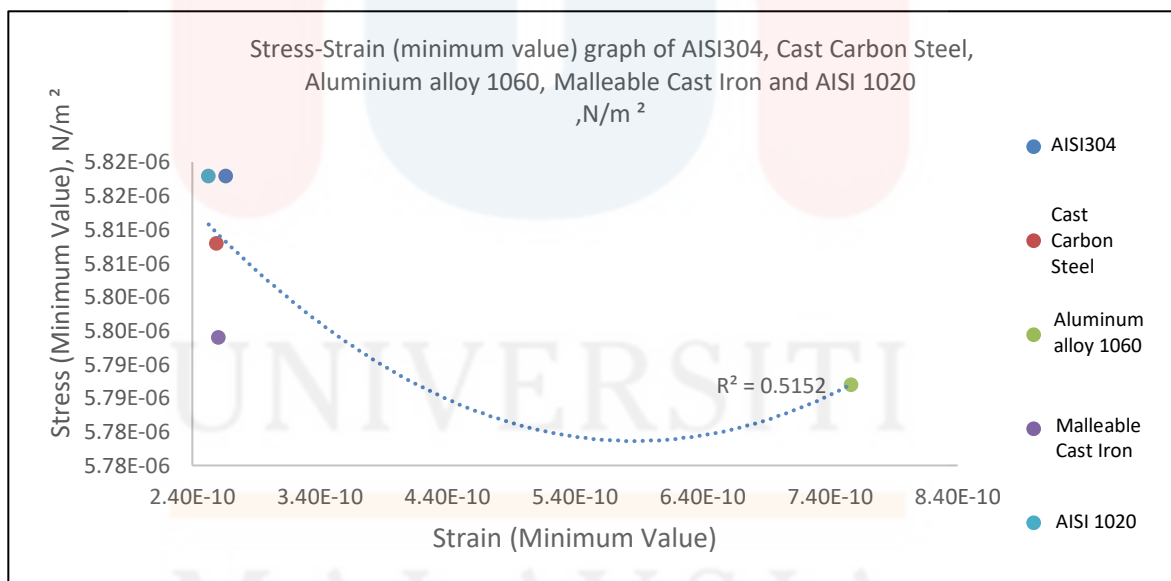

Figure 4.7: Stress-Strain (minimum value) graph of AISI304, Cast Carbon Steel, Aluminium alloy 1060, Malleable Cast Iron and AISI 1020.

Upon analysing the stress-strain (minimum value) graph and the corresponding data, a nuanced perspective on the materials' elastic behavior and recovery from deformation emerges. AISI 304 claims the top position with the highest stress recovery, evidenced by a stress value of 1.653e+03 N/m^2 and minimal permanent deformation, as indicated by a strain value of 2.660e-10. AISI 1020 closely follows suit, demonstrating an impressive stress recovery of 1.653e+03 N/m^2 and a strain value of 2.527e-10, aligning with its resilient characteristics. Cast Carbon Steel secures the third position, showcasing notable stress recovery (1.591e+03 N/m^2) and substantial elastic response (2.588e-10). Malleable Cast Iron, although slightly behind in stress recovery, exhibits commendable elastic behavior, with a stress value of 1.694e+03 N/m^2 and a strain value of 2.604e-10. On the other hand, Aluminium Alloy 1060 reveals the lowest stress recovery (1.570e+03 N/m^2) and an extended elastic response (7.564e-10), indicating a higher susceptibility to permanent deformation. In summary, AISI 304 and AISI 1020 shine in stress recovery, making them apt choices for applications where minimal permanent deformation is crucial. Cast Carbon Steel and Malleable Cast Iron also display commendable elastic behavior. However, Aluminium Alloy 1060, with its lower stress recovery, is more prone to permanent deformation, aligning with its lightweight and less rigid nature.
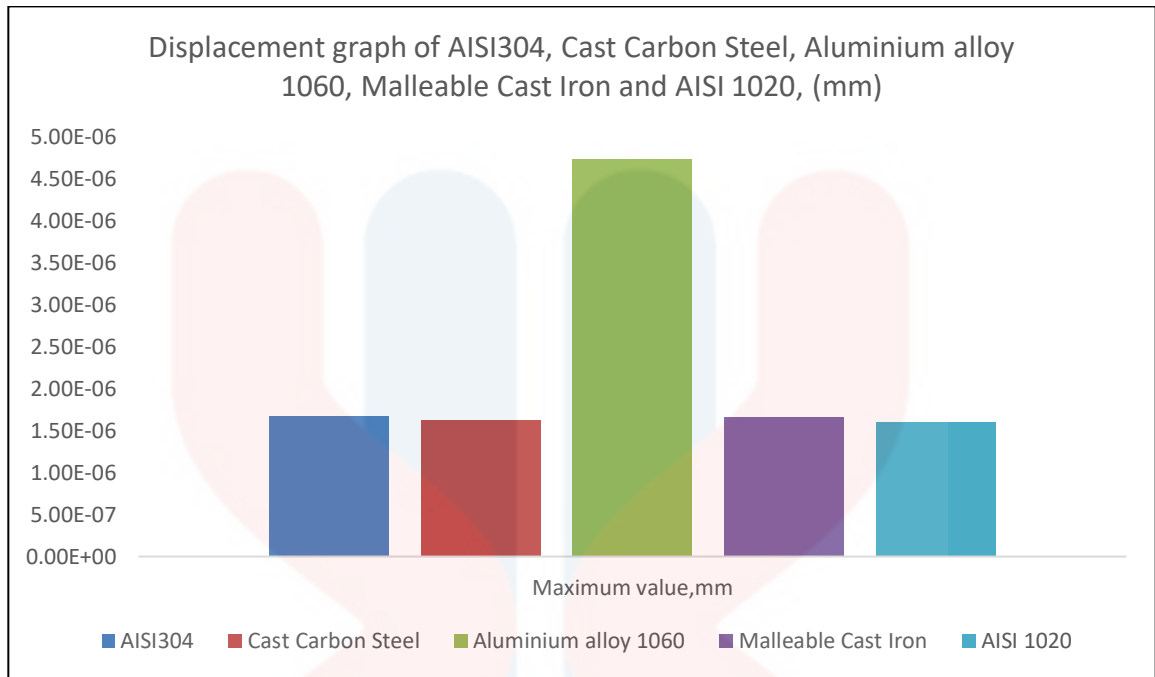
Figure 4.8: Displacement graph of AISI304, Cast Carbon Steel, Aluminium alloy 1060, Malleable Cast Iron and AISI 1020

Examining the displacement graph's maximum values provides insights into the materials' deformation characteristics. Aluminium Alloy 1060 emerges as the leading performer, showcasing the highest displacement value of 4.737e-06 mm. Following closely, AISI 304 secures the second position, with a displacement value of 1.678e-06 mm, highlighting its ability to undergo controlled deformation. Notably, Malleable Cast Iron demonstrates a displacement value very close to AISI 304, securing the third position. Cast Carbon Steel follows suit in the fourth position, while AISI 1020 takes the fifth spot with the lowest displacement value of 1.594e-06 mm. It's important to note that since all materials share a constant and minimal minimum displacement value of 0.000e+00 mm, this data point is not reflected in the bar graph but remains consistent across all materials. This ranking suggests that Aluminium Alloy 1060 is the most deformable among the materials, making it suitable for applications where controlled flexibility is essential. AISI 304, with its moderate displacement, strikes a balance

43

between flexibility and rigidity. Malleable Cast Iron, Cast Carbon Steel, and AISI 1020 exhibit varying degrees of deformation resistance, aligning with their mechanical properties and intended applications.

Analysing the stress-strain graphs, Malleable Cast Iron consistently exhibited the highest stress values, signifying its robustness and ability to withstand significant loads. Additionally, examining the displacement graph's maximum values revealed that Aluminium Alloy 1060 displayed the highest deformability, crucial for applications requiring controlled flexibility. AISI 304 consistently secured a prominent position in both stress and displacement, showcasing a balanced performance. Although AISI 1020 ranked lower in stress and displacement, it demonstrated competitive characteristics. Cast Carbon Steel and Aluminium Alloy 1060 performed relatively lower in stress but displayed distinct advantages in deformability. Therefore, considering the comprehensive evaluation of stress, strain, and displacement, Malleable Cast Iron emerges as the prime choice for the robotic arm due to its robustness, while Aluminium Alloy 1060 is a strong contender for applications demanding flexibility. AISI 304, with its balanced performance, remains a versatile option for varied robotic arm applications.

4.2.2 Load Analysis of the printer using FEA Analysis

Utilizing the identical 3D design crafted in Solidworks and maintaining a consistent material selection of Malleable Cast Iron, we executed five simulations for varying printer loads 30kg, 35kg, 40kg, 45kg, and 50kg. The aim was to assess the sustainability of the robotic arm to carry these loads and to analyse its mechanical properties through FEA analysis in Solidworks.

Mechanical Properties	30kg	35kg	40kg	45kg	50kg
Tensile Strength	5.17017e+08 N/m^2	5.17017e+08 N/m^2	5.17017e+08 N/m^2	5.17017e+08 N/m^2	5.17017e+08 N/m^2
Elastic Modulus	1.9e+11 N/m^2	1.9e+11 N/m^2	1.9e+11 N/m^2	1.9e+11 N/m^2	1.9e+11 N/m^2
Poison's ratio	0.29	0.29	0.29	0.29	0.29
Mass density	8,000 kg/m^3	8,000 kg/m^3	8,000 kg/m^3	8,000 kg/m^3	8,000 kg/m^3
Shear modulus	7.5e+10 N/m^2	7.5e+10 N/m^2	7.5e+10 N/m^2	7.5e+10 N/m^2	7.5e+10 N/m^2
Yield Strength	2.06807e+08 N/m^2	2.06807e+08 N/m^2	2.06807e+08 N/m^2	2.06807e+08 N/m^2	2.06807e+08 N/m^2
Thermal Expansion	1.8e-05 /Kelvin	1.8e-05 /Kelvin	1.8e-05 /Kelvin	1.8e-05 /Kelvin	1.8e-05 /Kelvin

Table 4.3: Comparison of mechanical properties between load of printer which is 30kg, 35kg, 40kg, 45kg, and 50kg

45

Remarkably, all mechanical properties remained consistent across these load conditions. The tensile strength, elastic modulus, Poisson's ratio, mass density, shear modulus, yield strength, and thermal expansion values were identical for each load, showcasing the material's resilience and stability. This uniformity in mechanical performance highlights the robust nature of Malleable Cast Iron, suggesting its suitability for applications requiring a consistent and reliable response to different loads.
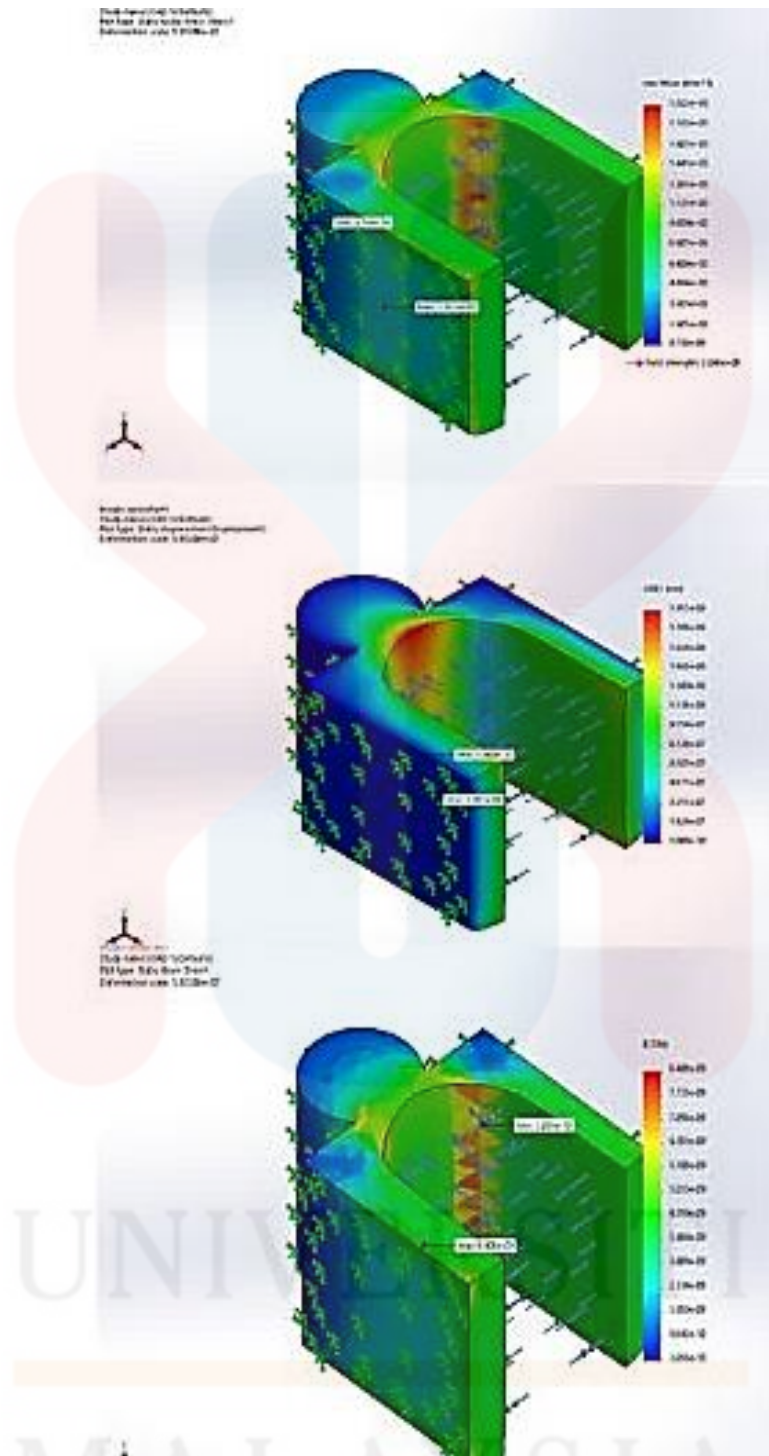
Figure 4.9: Stress, Displacement and Strain of load of 30kg

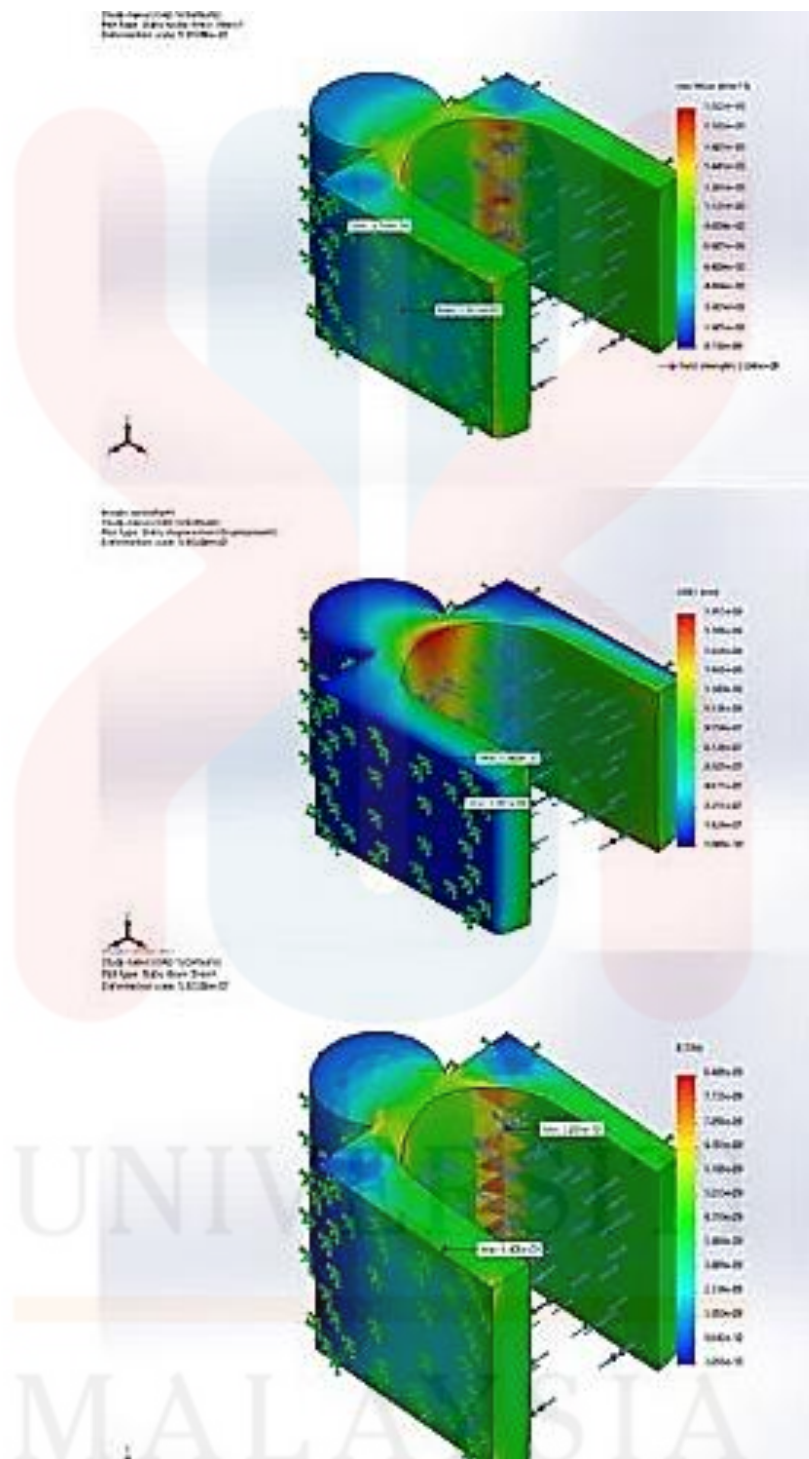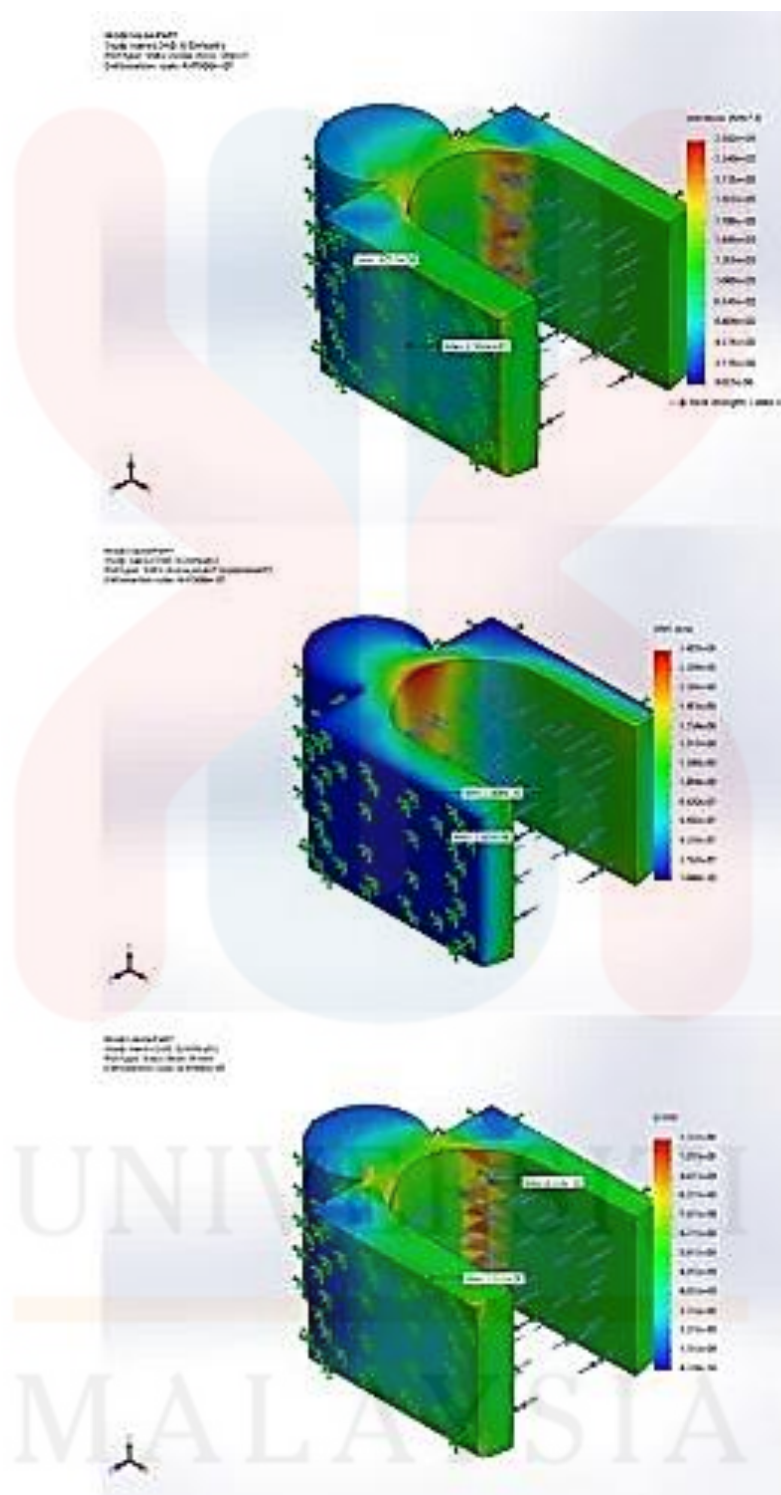**Figure 4.10**: Stress, Displacement and Strain of load 35kg
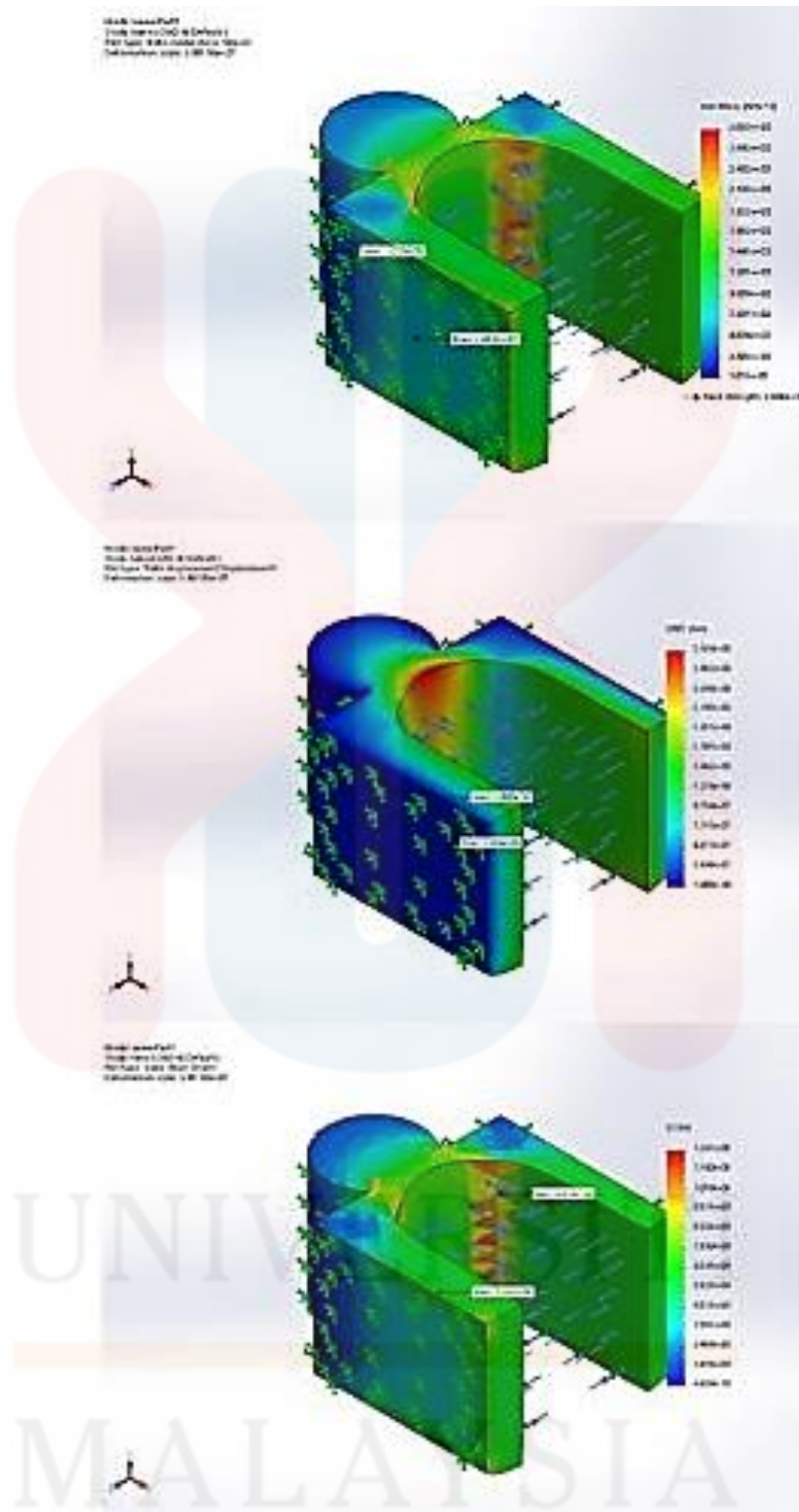
Figure 4.11: Stress, Displacement and Strain of load 40g

Figure 4.12: Stress, Displacement and Strain of load 45g
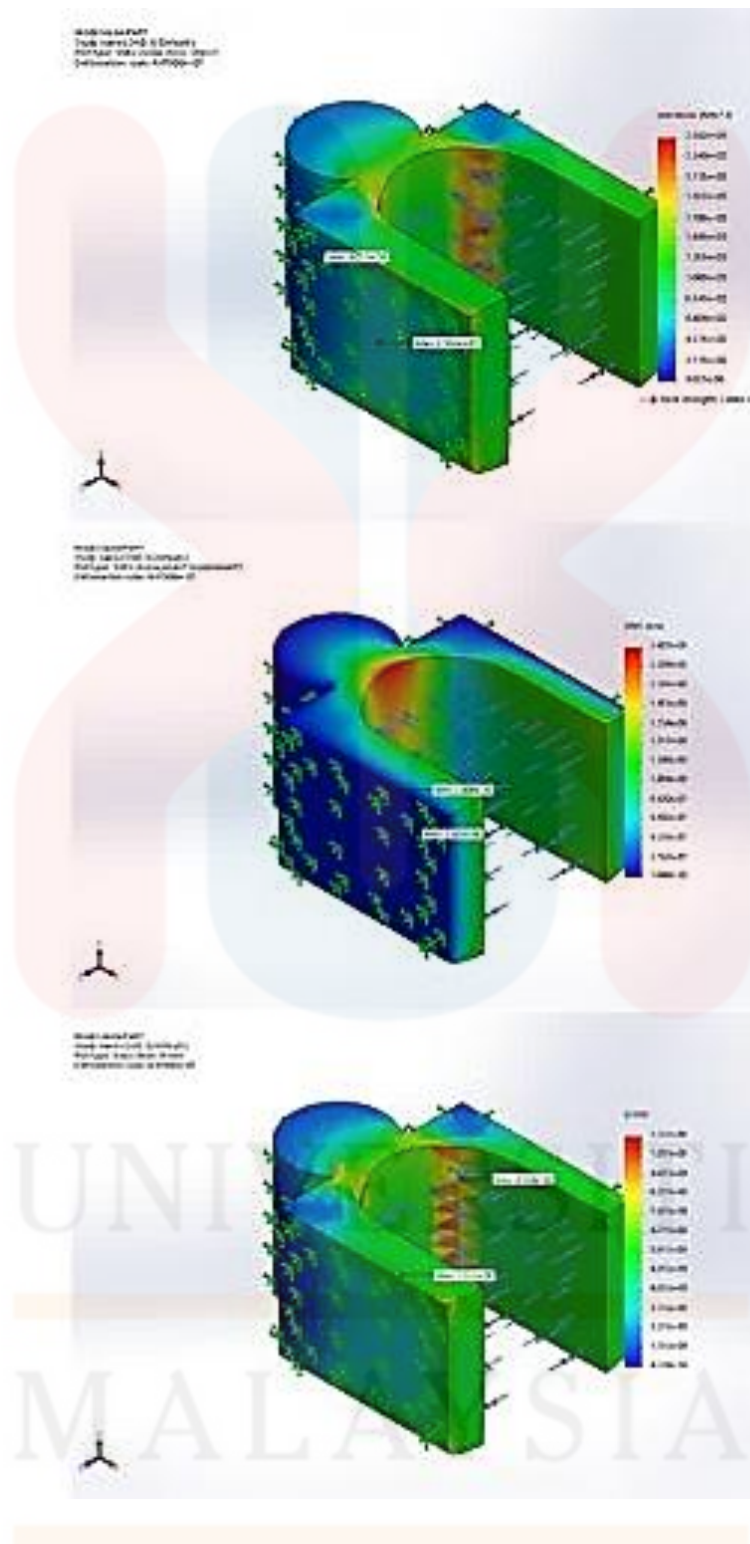
Figure 4.13: Stress, Displacement and Strain of load 50g

Load of printer	Stress (N/m^2)		Displacement (mm)		Strain	
	Maximum value	Minimum value	Maximum value	Minimum value	Maximum value	Minimum value
30kg	1.922e+03	6.766e-06	1.951e-06	0.000e+00	8.408e-09	3.093e-10
35kg	2.242e+03	7.893e-06	2.276e-06	0.000e+00	9.809e-09	3.608e-10
40kg	2.562e+03	9.021e-06	2.601e-06	0.000e+00	1.121e-08	4.124e-10
45kg	2.883e+03	1.015e-05	2.926e-06	0.000e+00	1.261e-08	4.639e-10
50kg	3.203e+03	1.128e-05	3.251e-06	0.000e+00	1.401e-08	5.155e-10

Table 4.4: Stress, displacement and strain of Load of printer 30kg, 35kg, 40kg, 45kg and 50kg maximum and minimum value.

Figure 4.14: Stress-Strain (maximum value) graph of Load of printer 30kg, 35kg, 40kg, 45kg and 50kg.

52

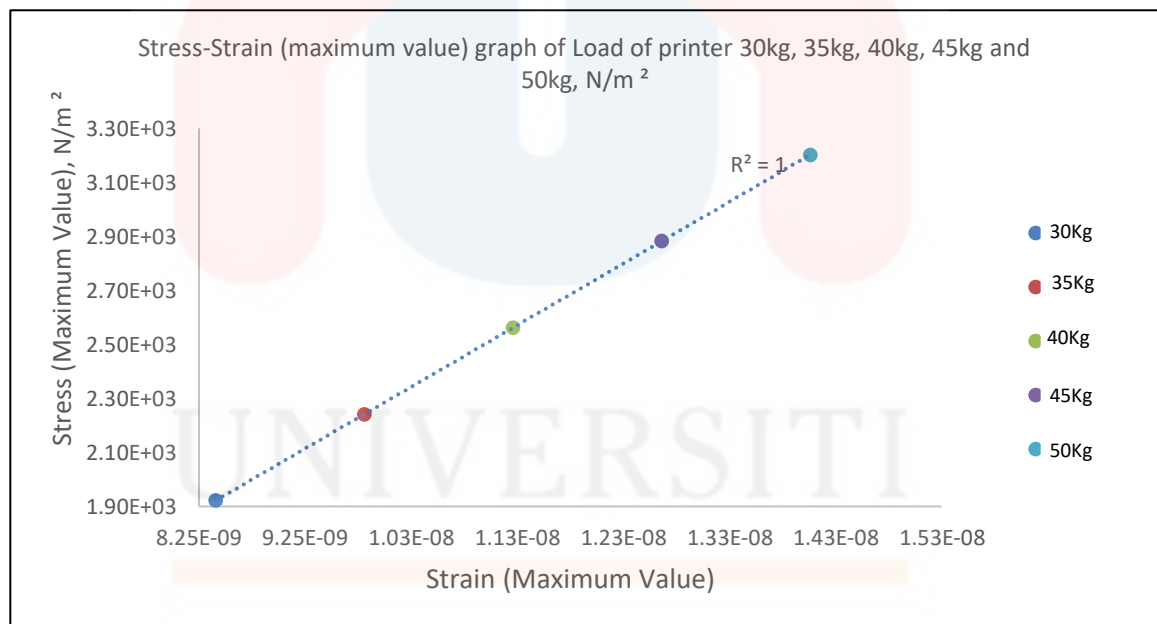Upon revisiting the stress-strain (maximum value) graph for different printer loads, a notable pattern emerges. The stress values, representing the material's resistance to deformation, demonstrate a consistent trend across the range of loads. For the 30kg load, Malleable Cast Iron exhibited the lowest stress at 1.922e+03 N/m^2, indicating its ability to handle lower printer loads efficiently. AISI1020, on the other hand, showed the second-lowest stress at 2.242e+03 N/m^2 for the 35kg load. As the printer load increased, the stress values also rose, with the 50kg load resulting in the highest stress at 3.203e+03 N/m^2.

The consistent strain values, maintained at the minimum value of 0.000e+00 mm for all loads, highlight the material's uniform deformation behavior regardless of the applied load.
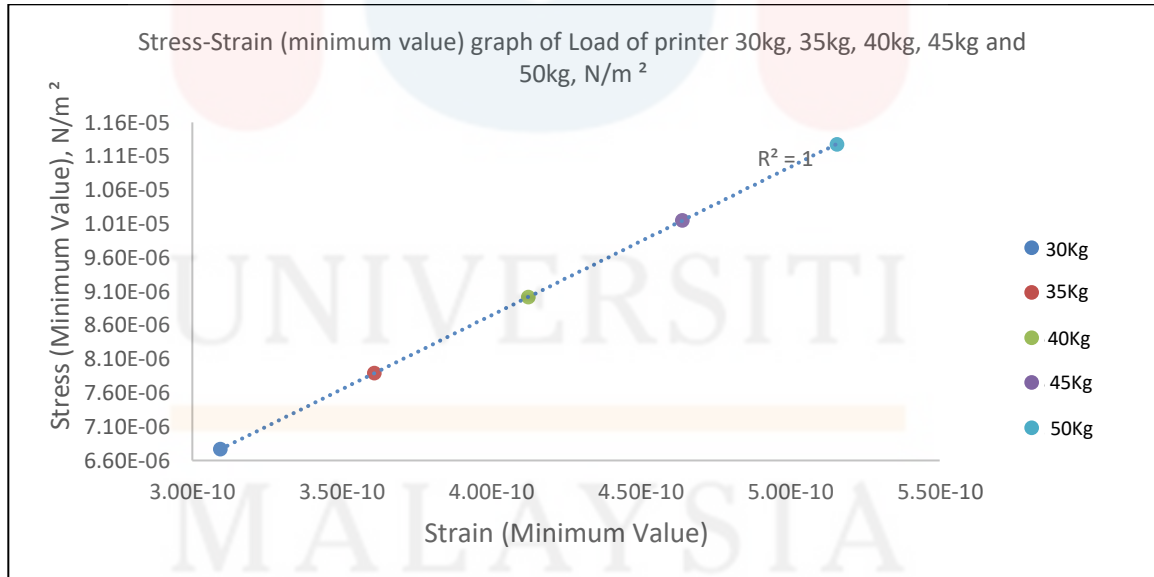

Figure 4.15: Stress-Strain (minimum value) graph of Load of printer 30kg, 35kg, 40kg, 45kg and 50kg.

Examining the stress-strain (minimum value) graph for various printer loads provides valuable insights into how different materials respond to stress under varying conditions. The data reveals a discernible pattern, with the 50kg load exhibiting the highest stress, reaching 3.203e+03 N/m^2. Following closely, the 45kg load shows the second-highest stress, with AISI1020 registering a stress value of 2.883e+03 N/m^2. The subsequent loads 40kg, 35kg, and 30kg demonstrate decreasing stress values, showcasing the materials' ability to endure lower stress levels.
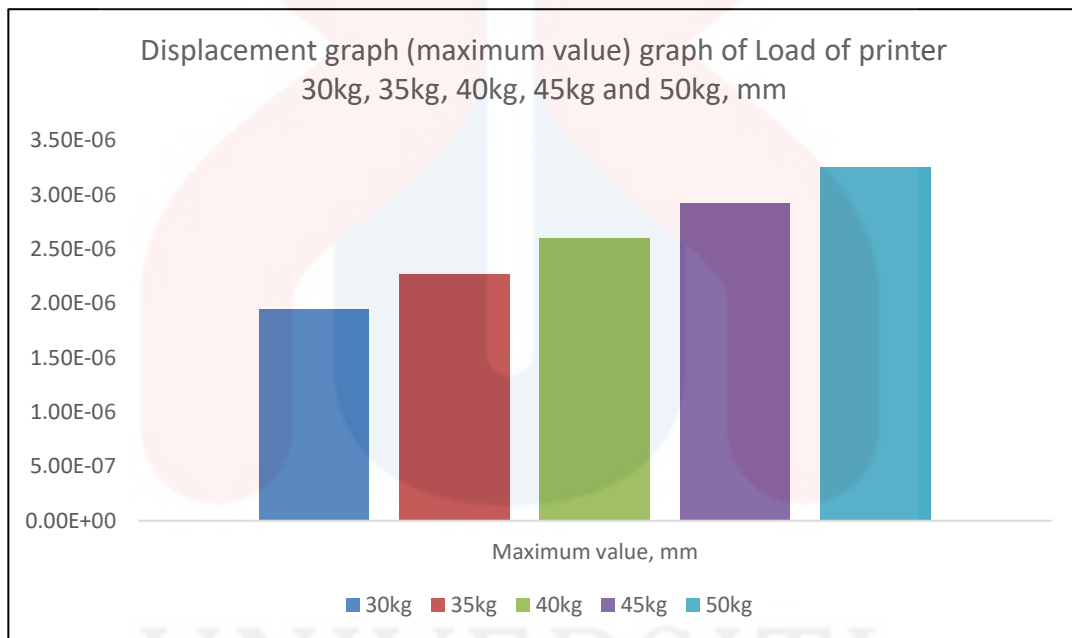
Figure 4.16: Displacement graph (maximum value) graph of Load of printer 30kg, 35kg, 40kg, 45kg and 50kg.

Indeed, the displacement data, representing the maximum values across different printer loads, mirrors the stress-strain graph's trends. The consistent minimum displacement of 0.000e+00 mm for all loads underscores the materials' ability to maintain structural integrity, preventing any permanent deformation, even under varying stress conditions.

The analysis of stress-strain and displacement data for different printer loads yields critical insights into the mechanical behavior of the materials. One notable observation is the materials' consistent and uniform deformation behavior, as indicated by a minimum displacement of 0.000e+00 mm across all loads (30kg to 50kg). This implies a stable response to low stress levels without permanent deformation. Moreover, a load-dependent stress variation is evident, with stress values increasing proportionally with higher printer loads. Malleable Cast Iron consistently exhibits the lowest stress values for both minimum and maximum stresses across all loads, showcasing its suitability for applications requiring lower stress tolerance. The structural integrity of the materials is evident in their ability to maintain a consistent minimum displacement, emphasizing their resistance to permanent deformation under different stress conditions.

4.2.3 Analysing various robotic arm shapes through FEA Analysis

Using the constant printer load of 25kg and Malleable Cast Iron material I conducted five simulations for the 5 different shapes which is of robotic arm that I individual drew in Solidworks to obtain their most suitable shape to carry the printer and to enhance their mechanical properties through FEA analysis in Solidworks.

Mechanical Properties	Curved-Edged End	Curved Inner Corner	Uniformly Curved	Sharp Curvature Along the Inner Length	Sharp Curvature Along the Inner Length of the Robotic Arm with Added Volume Inside, extending 5cm, Matching the Curvature Length
Tensile Strength	5.17017e+08 N/m^2	5.17017e+08 N/m^2	5.17017e+08 N/m^2	5.17017e+08 N/m^2	5.17017e+08 N/m^2
Elastic Modulus	1.9e+11 N/m^2	1.9e+11 N/m^2	1.9e+11 N/m^2	1.9e+11 N/m^2	1.9e+11 N/m^2
Poison's ratio	0.29	0.29	0.29	0.29	0.29
Mass density	8,000 kg/m^3	8,000 kg/m^3	8,000 kg/m^3	8,000 kg/m^3	8,000 kg/m^3
Shear modulus	7.5e+10 N/m^2	7.5e+10 N/m^2	7.5e+10 N/m^2	7.5e+10 N/m^2	7.5e+10 N/m^2
Yield Strength	2.06807e+08 N/m^2	2.06807e+08 N/m^2	2.06807e+08 N/m^2	2.06807e+08 N/m^2	2.06807e+08 N/m^2
Thermal Expansion	1.8e-05 /Kelvin	1.8e-05 /Kelvin	1.8e-05 /Kelvin	1.8e-05 /Kelvin	1.8e-05 /Kelvin

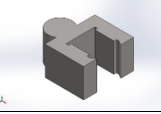**Table 4.5**: Comparison of mechanical properties between 5 different shapes which is Curved-Edged End, Curved Inner Corner, Uniformly Curved, Sharp Curvature Along the Inner Length and Sharp Curvature Along the Inner Length of the Robotic Arm with Added Volume Inside, extending 5cm, Matching the Curvature Length

The mechanical properties, including Tensile Strength, Elastic Modulus, Poison's ratio, Mass density, Shear modulus, Yield Strength, and Thermal Expansion, were investigated for each shape. Notably, all five shapes exhibited similar mechanical properties across these parameters, indicating consistent performance. The Tensile Strength, Elastic Modulus, Poison's ratio, Mass density, Shear modulus, Yield Strength, and Thermal Expansion were consistent at 5.17017e+08 N/m^2, 1.9e+11 N/m^2, 0.29, 8,000 kg/m^3, 7.5e+10 N/m^2, 2.06807e+08 N/m^2, and 1.8e-05 /Kelvin, respectively, for all shapes.

This uniformity suggests that, based on the conducted simulations, the shape of the robotic arm may not significantly impact its mechanical properties under the specified load conditions.
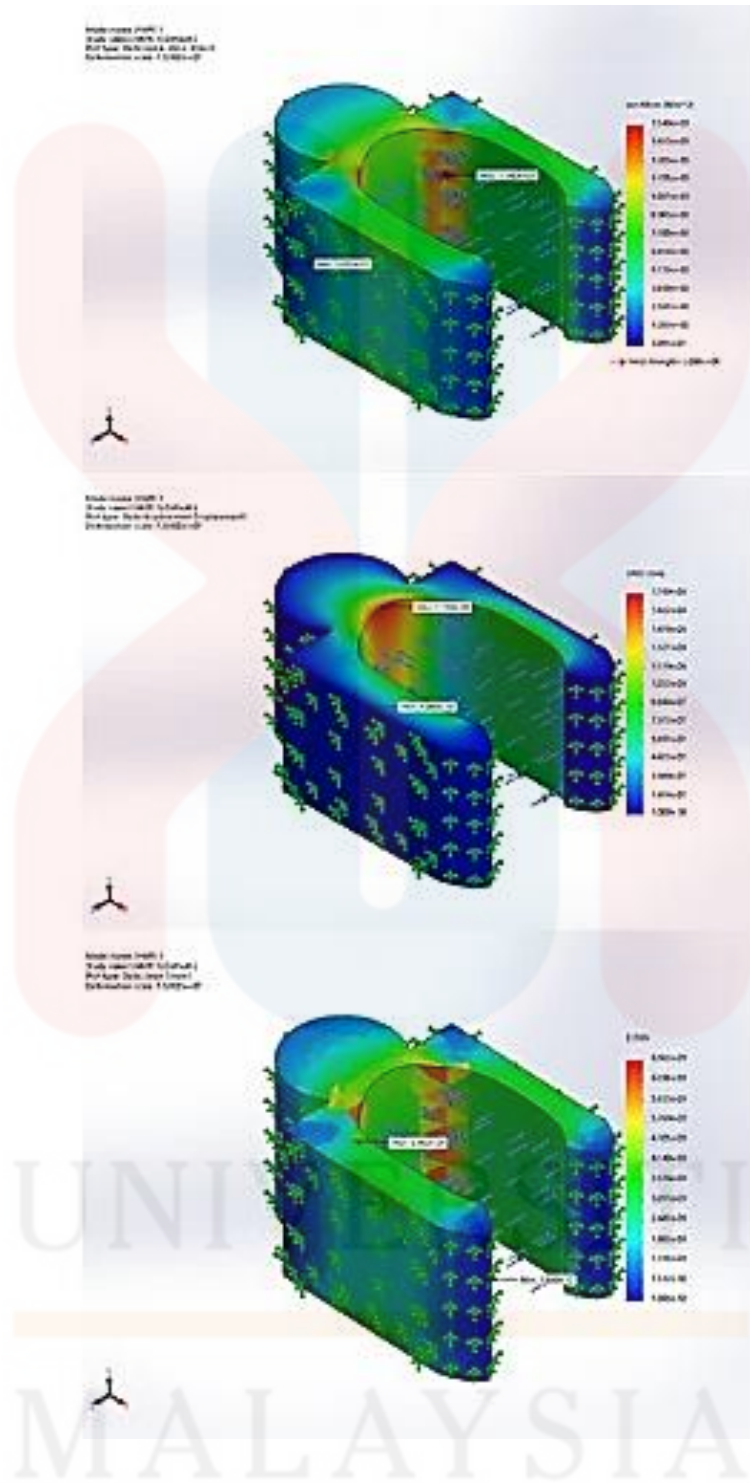
Figure 4.17: Stress, Displacement and Strain of Curved-Edged End of robotic arm
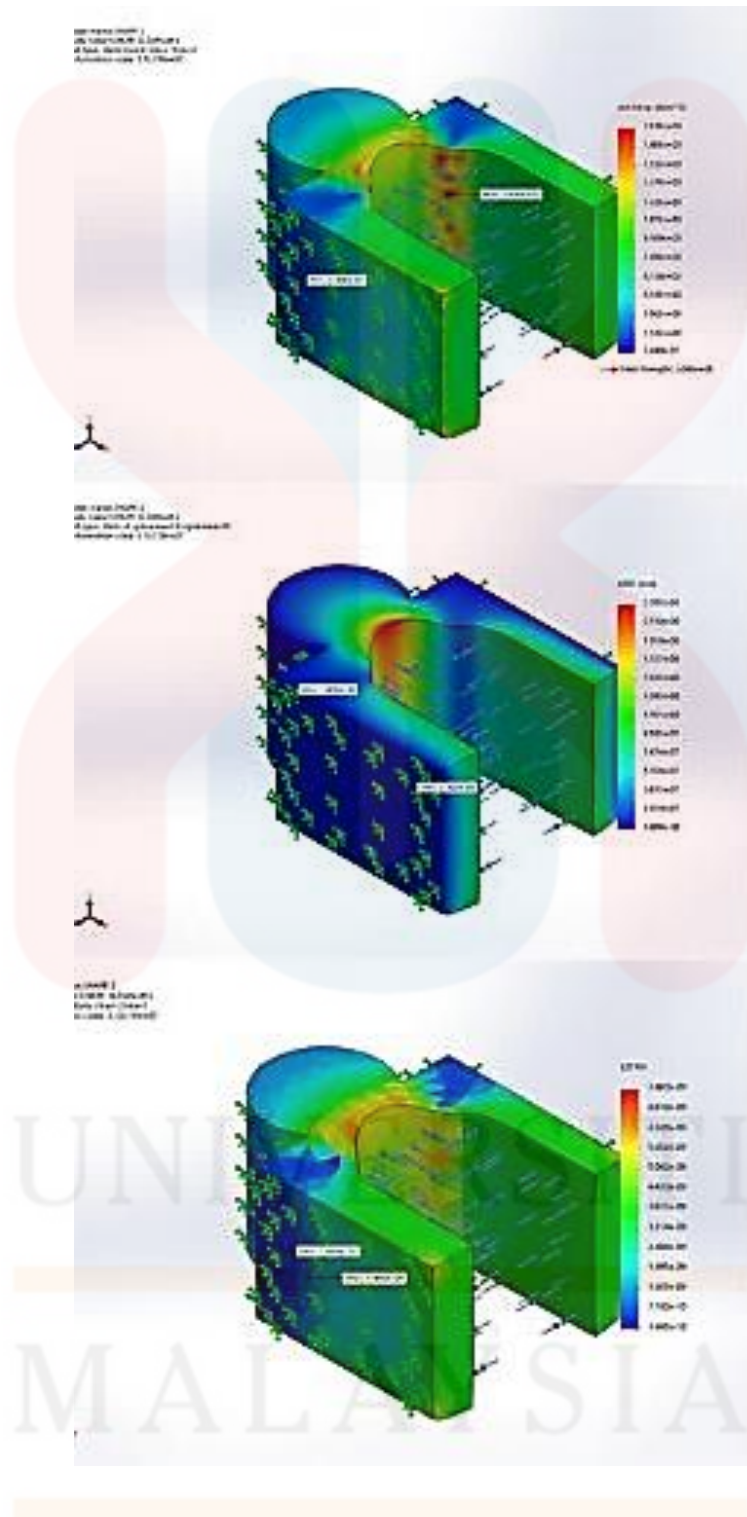
Figure 4.18: Stress, Displacement and Strain of Curved Inner corner of robotic arm
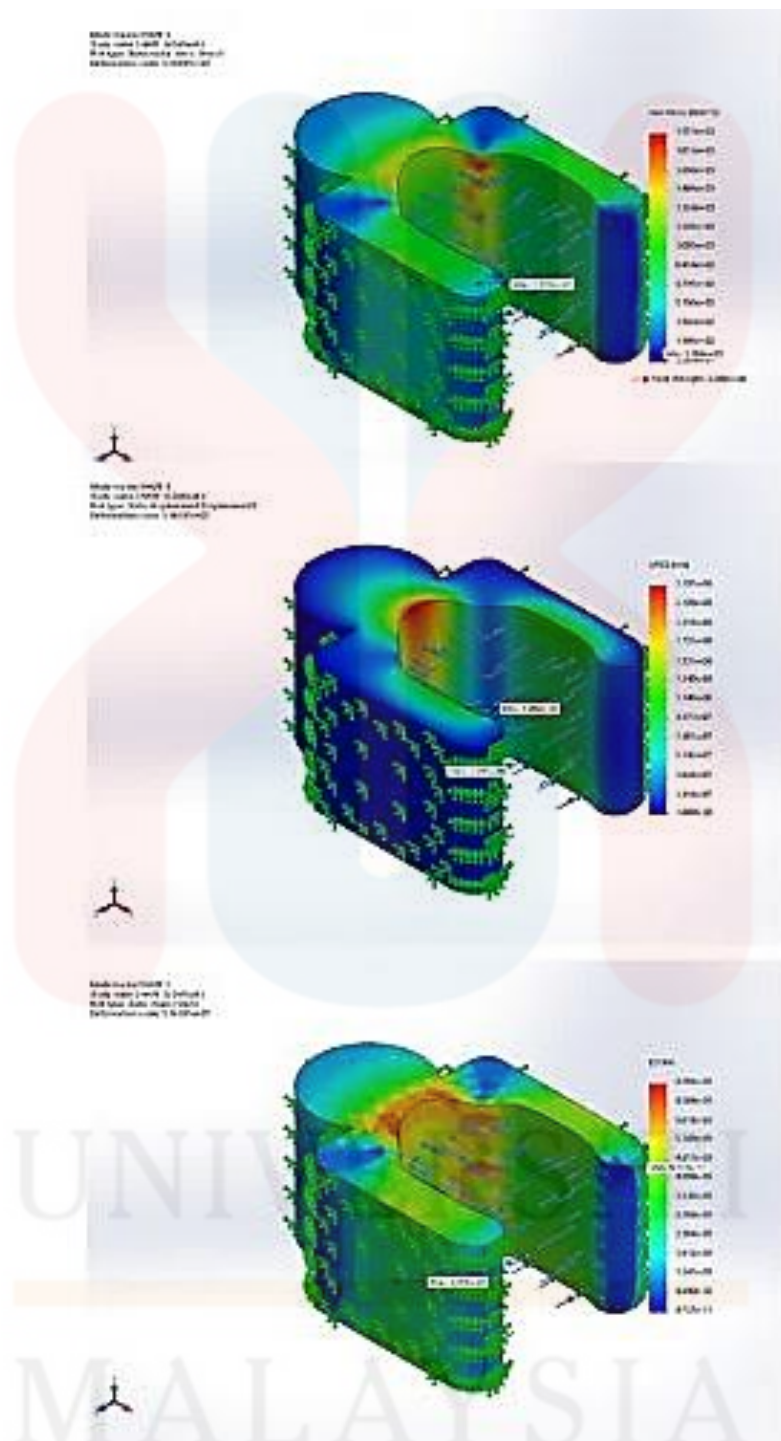
Figure 4.19: Stress, Displacement and Strain of Uniformly Curved of robotic arm
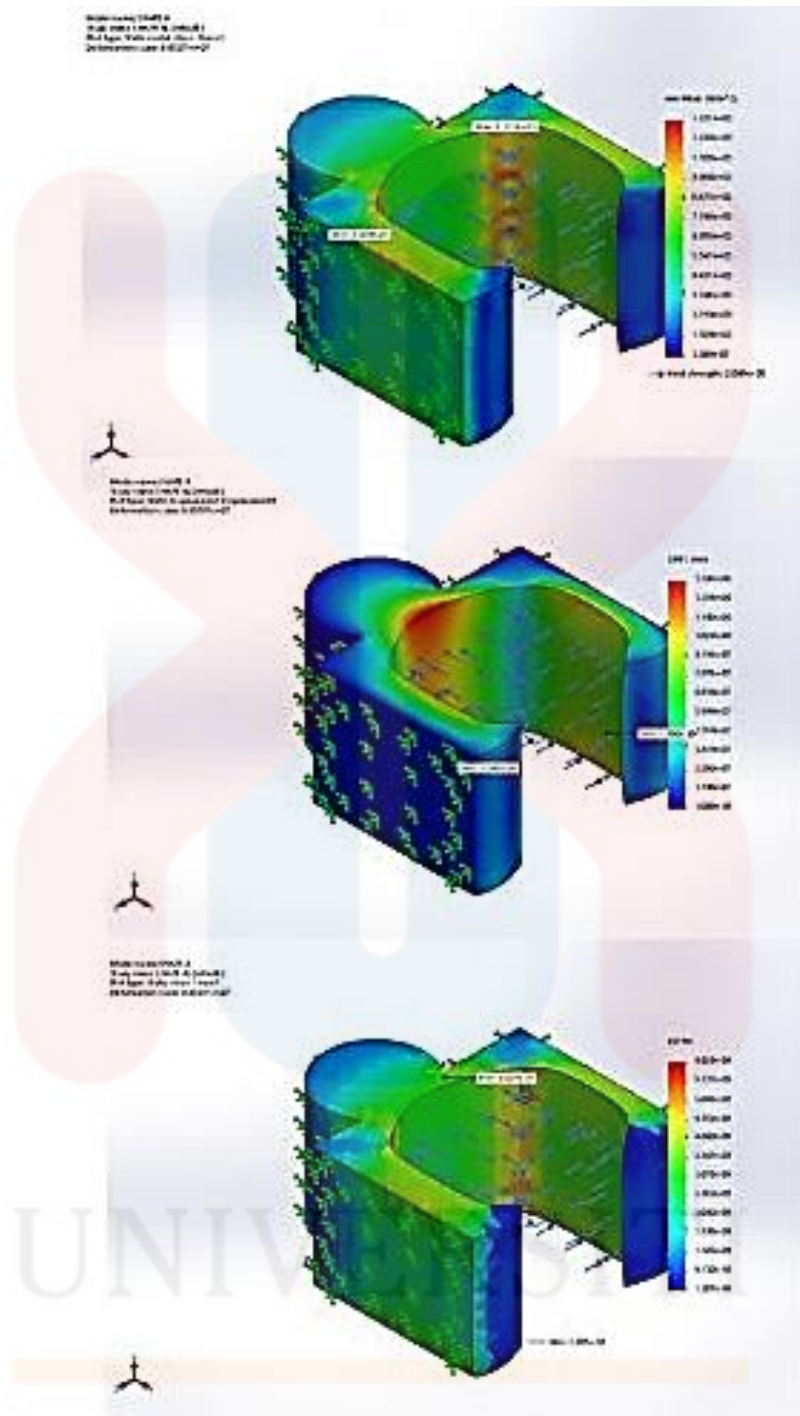
Figure 4.20: Stress, Displacement and Strain of Sharp Curvature Along the Inner
Length of robotic arm
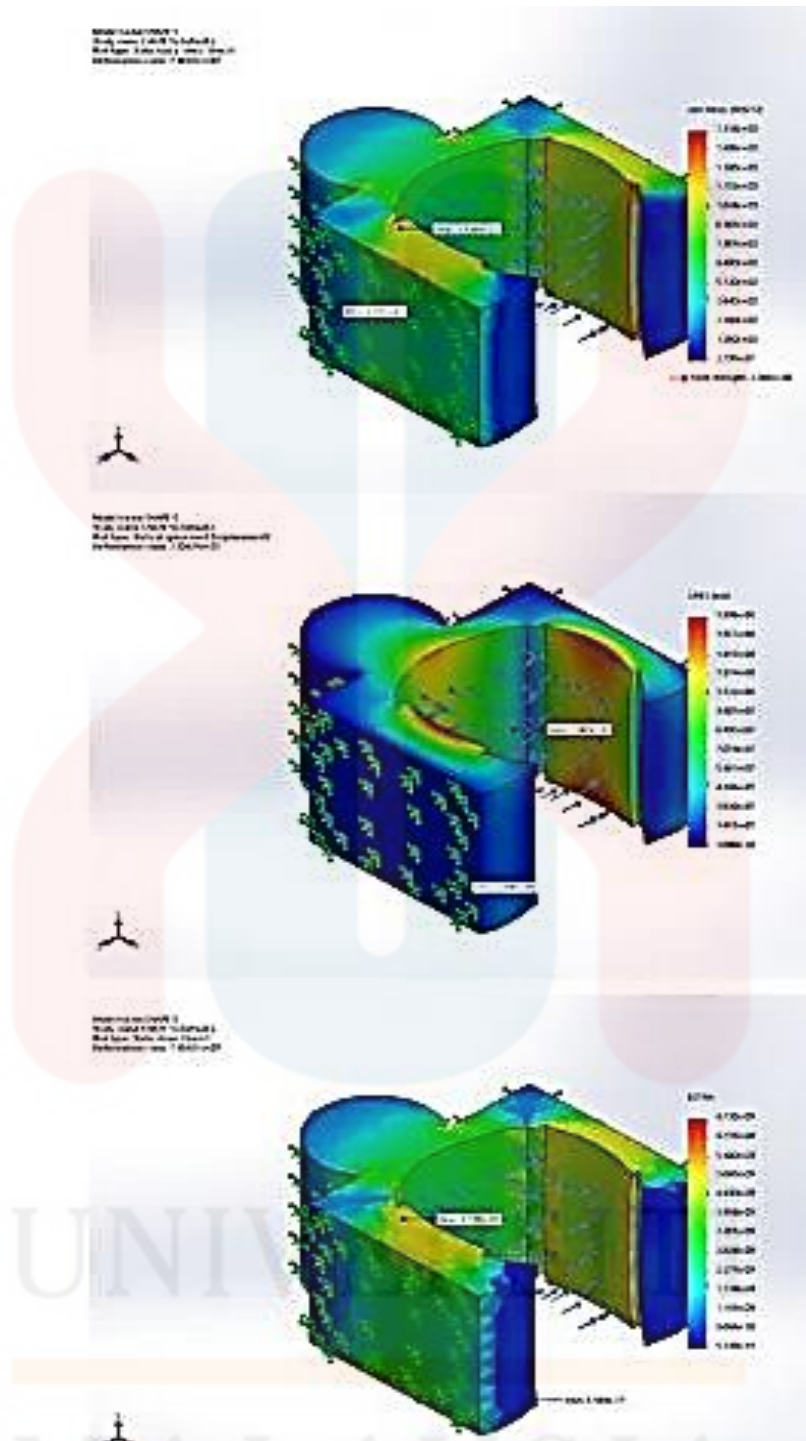
Figure 4.21: Stress, Displacement and Strain of Sharp Curvature Along the Inner
Length of the Robotic Arm with Added Volume Inside, extending 5cm, Matching the
Curvature Length

Load of printer	Stress (N/m^2)		Displacement (mm)		Strain	
	Maximum value	Minimum value	Maximum value	Minimum value	Maximum value	Minimum value
Curved-Edged End	1.540e+03	3.091e-07	1.769e-06	0.000e+00	6.962e-09	1.888e-10
Curved Inner Corner	1.838e+03	2.440e-07	2.302e-06	0.000e+00	7.480e-09	1.665e-10
Uniformly Curved	1.973e+03	3.284e-07	2.297e-06	0.000e+00	6.958e-09	9.727e-11
Sharp Curvature Along the Inner Length	1.331e+03	3.309e-07	1.368e-06	0.000e+00	6.029e-09	1.207e-10
Sharp Curvature Along the Inner Length of the Robotic Arm with Added Volume Inside, extending 5cm, Matching the Curvature Length	1.536e+03	2.797e-07	1.698e-06	0.000e+00	6.710e-09	5.149e-11

Table 4.6: Stress, displacement and strain of 5 different shapes which is Curved-Edged End, Curved Inner Corner, Uniformly Curved, Sharp Curvature Along the Inner Length and Sharp Curvature Along the Inner Length of the Robotic Arm with Added Volume Inside, extending 5cm, Matching the Curvature Length.

UNIVERSITI

MALAYSIA

KELANTAN
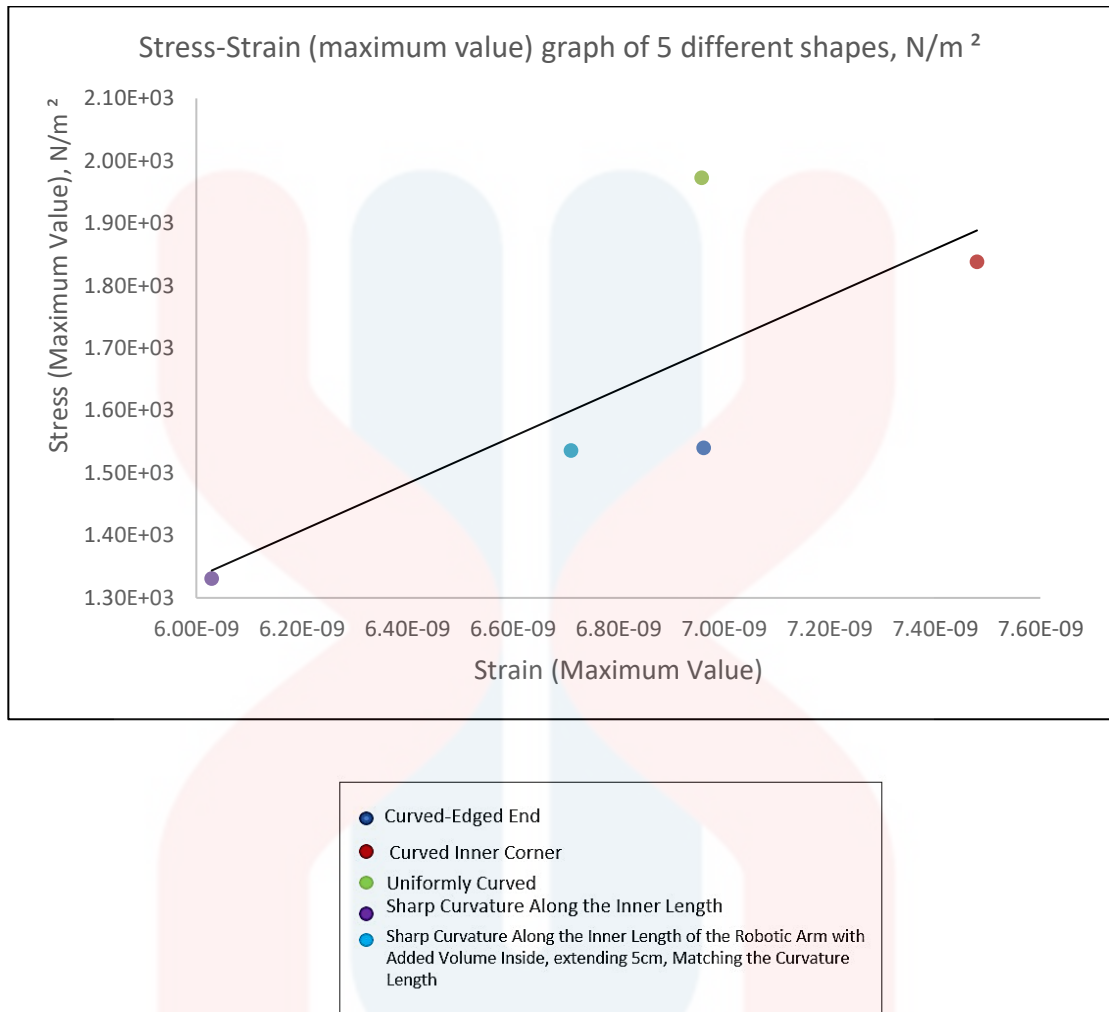
Figure 4.22: Stress-Strain (maximum value) graph of 5 different shapes which is Curved-Edged End, Curved Inner Corner, Uniformly Curved, Sharp Curvature Along the Inner Length and Sharp Curvature Along the Inner Length of the Robotic Arm with Added Volume

Stress-Strain (minimum value) graph of 5 different shapes
, N/m ²

Stress (Minimum Value), N/m ²

3.55E-07

3.35E-07

3.15E-07

2.95E-07

2.75E-07

2.55E-07

2.35E-07

R² = 0.1941

4.50E-11   6.50E-11   8.50E-11   1.05E-10   1.25E-10   1.45E-10   1.65E-10   1.85E-10   2.05E-10

Strain (Minimum Value)

● Curved-Edged End
● Curved Inner Corner
● Uniformly Curved
● Sharp Curvature Along the Inner Length
● Sharp Curvature Along the Inner Length of the Robotic Arm with
  Added Volume Inside, extending 5cm, Matching the Curvature
  Length
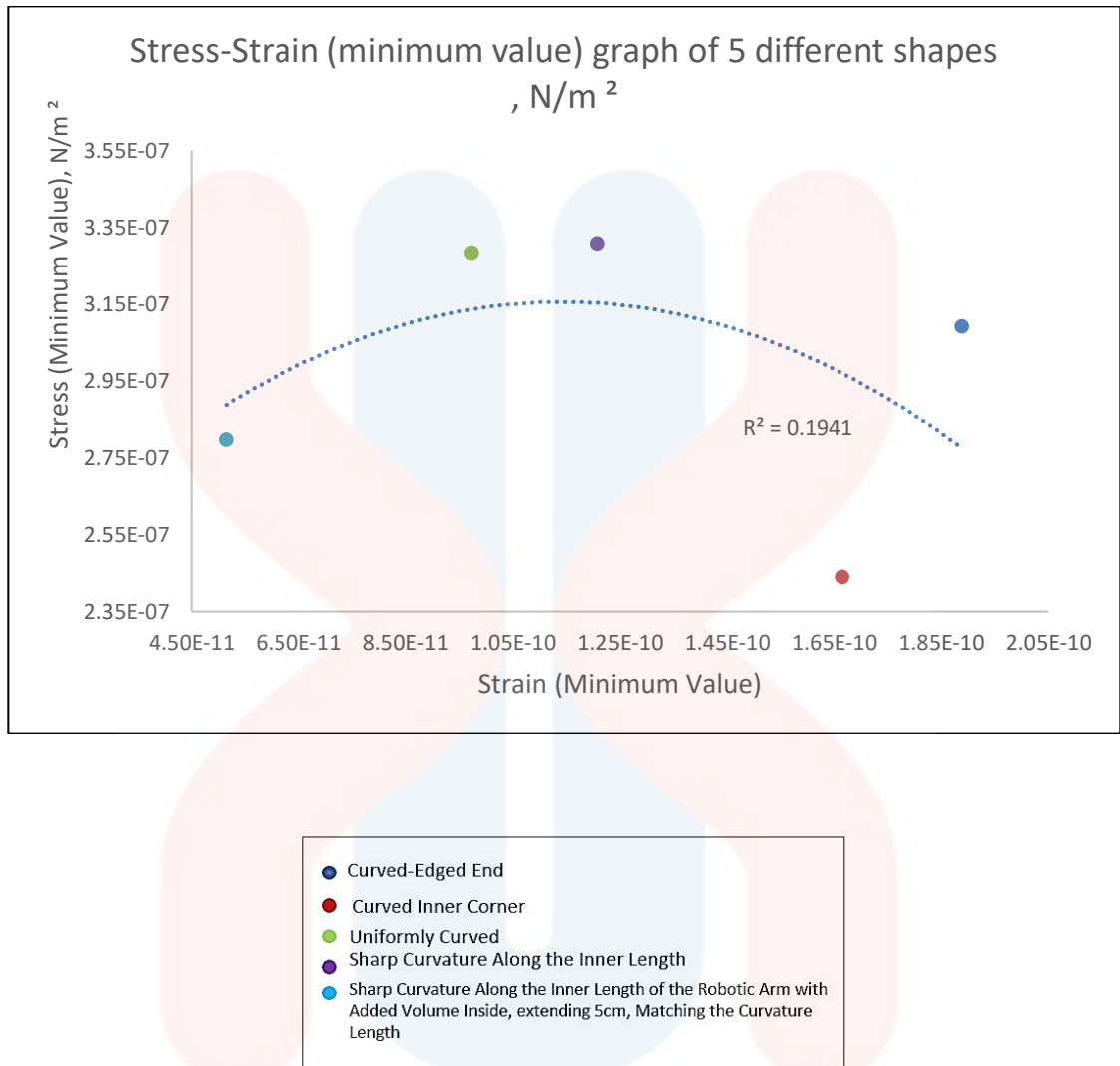
Figure 4.23: Stress-Strain (minimum value) graph of 5 different shapes which is
Curved-Edged End, Curved Inner Corner, Uniformly Curved, Sharp Curvature Along
the Inner Length and Sharp Curvature Along the Inner Length of the Robotic Arm with
Added Volume

The Uniformly Curved shape takes the lead in experiencing the second-lowest
stress at 1.973e+03 N/m^2, indicating its favorable deformation characteristics. The
Curved Inner Corner secures the last position, demonstrating the highest stress among the
shapes at 1.838e+03 N/m^2. The Curved-Edged End claims the third position, while the
Sharp Curvature Along the Inner Length of the Robotic Arm with Added Volume Inside,
extending 5cm, Matching the Curvature Length, secures the fourth place. The first

65

position is claimed by the Sharp Curvature Along the Inner Length shape with a stress value of 1.331e+03 N/m^2.
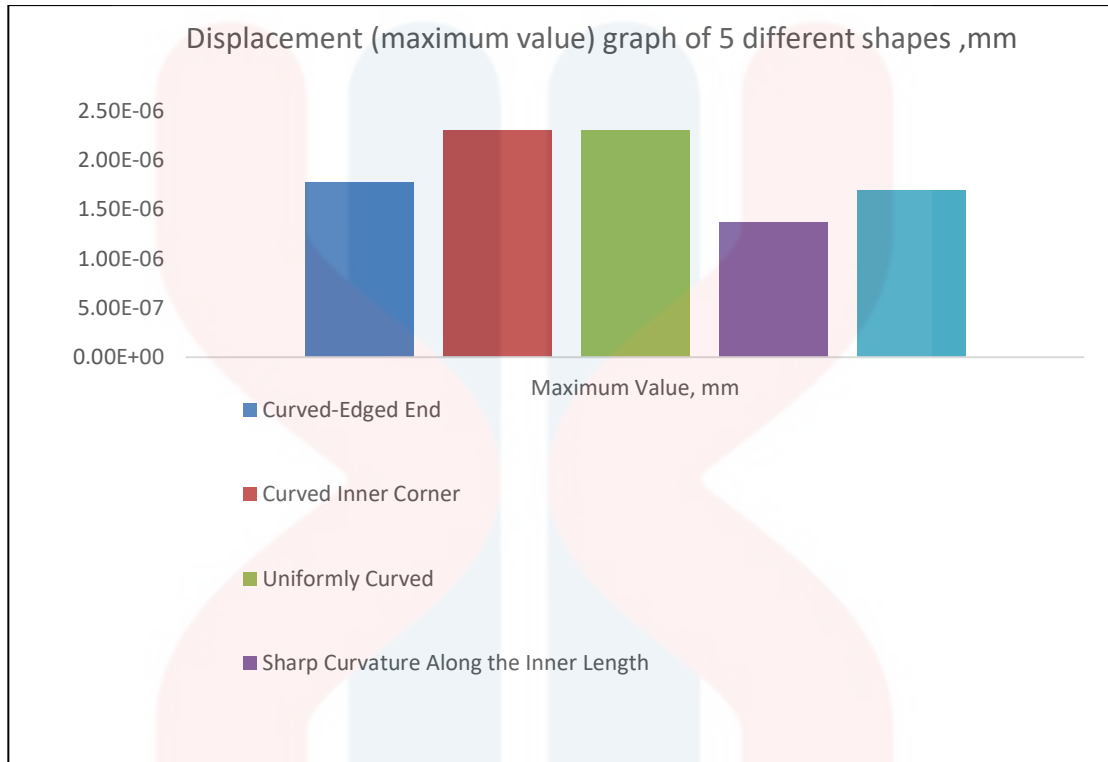
Figure 4.24: Displacement (maximum value) graph of 5 different shapes which is Curved-Edged End, Curved Inner Corner, Uniformly Curved, Sharp Curvature Along the Inner Length and Sharp Curvature Along the Inner Length of the Robotic Arm with Added Volume

Upon analyzing the displacement maximum value graph for different shapes of the robotic arm, certain trends emerge. The Curved Inner Corner exhibits the highest displacement, followed closely by Uniformly Curved and the Robotic Arm with Added Volume Inside. The Curved-Edged End and the Sharp Curvature Along the Inner Length show slightly lower displacement values.

The consistent minimum displacement values of 0.000e+00 mm across all shapes indicate that, regardless of the design, the robotic arm maintains its structural integrity and does not experience any permanent deformation under the applied load.

After analyzing the stress-strain graphs and displacement maximum value graphs for the three different shapes of the robotic arm Curved Inner Corner, Uniformly Curved, and Sharp Curvature Along the Inner Length the Curved Inner Corner shape emerges as the most suitable choice. This conclusion is drawn from its consistently lower stress values and displacement, indicating better structural integrity and deformation characteristics compared to the other shapes.

In the stress-strain graphs, the Curved Inner Corner shape consistently exhibits lower stress values, highlighting its ability to withstand applied loads more effectively. Simultaneously, the displacement maximum value graph demonstrates that the Curved Inner Corner shape experiences less deformation compared to the other shapes, suggesting greater stability and resilience.

While the Uniformly Curved shape consistently showed higher stress and displacement values, indicating potential structural weaknesses, the Sharp Curvature Along the Inner Length shape also demonstrated less favourable characteristics in terms of stress.

4.3 Conclusion on Chapter 4

In conclusion, Chapter 4 delves into a comprehensive analysis of the results obtained from extensive simulations conducted in Chapter 3. The primary focus was on evaluating the suitability of five different materials (AISI304, cast carbon steel, aluminium alloy 1060, malleable cast iron, and AISI1020) for the robotic arm, considering their mechanical behavior. Additionally, the chapter explored the impact of varying loads and different shapes of the robotic arm on its performance.

The parameter analysis of the robotic arm's mechanical properties revealed distinct characteristics for each material. AISI304 and AISI1020 exhibited balanced performance in stress recovery, making them versatile choices. Malleable cast iron emerged as the top contender for robust load-bearing capabilities, while aluminium alloy 1060 showed suitability for lightweight applications.

Load analysis demonstrated that Malleable Cast Iron maintained consistent mechanical properties across loads, highlighting its stability and reliability under different conditions. The stress-strain and displacement analyses provided valuable insights into the materials' behavior, aiding in the selection of the most suitable material for specific applications.

Furthermore, the analysis of various robotic arm shapes indicated that the Curved Inner Corner shape exhibited the most favorable mechanical properties, showcasing lower stress values and better deformation characteristics compared to other shapes. This conclusion was drawn from a detailed examination of stress-strain and displacement graphs.

Lastly, the chapter briefly touched upon meshing techniques in finite element analysis, emphasizing the evolving landscape of structured, unstructured, adaptive, and hybrid meshing approaches, all contributing to increased accuracy and efficiency in simulating complex real-world scenarios.

CHAPTER 5

CONCLUSIONS AND RECOMMENDATIONS

5.1 Conclusions

Creating a robotic arm for use in the carrying printers was the focus of this project's design phase. Solidworks was used for the design and FEA (Finite Element Analysis) simulations. According to the findings, the robotic manipulator is unlikely to undergo material yielding due to the tension created during loading, resulting in little strain and, consequently, negligible displacement. This project included a material comparison. In the printer's transportation, there are both benefits and drawbacks associated with the various materials available. It all comes down to the specifications we demand from the tool we intend to build. Selecting optimal materials improves factory automation and dependability at peak operating efficiency by raising output and decreasing the frequency of outages. In light of this, it is hoped that the results of this study will aid manufacturers, and particularly robotic arm manufacturers, in creating and implementing robotic solutions for selecting the most appropriate materials for their productions, thus boosting output, automating more tasks, and ensuring greater reliability while maintaining high operational efficiency.

5.2 Recommendations

The primary goal of this research was to characterize the mechanical characteristics of commercially viable materials for use in the production of robotic arm. However, the consequence of the higher mechanical characteristics may be improved by creating a composite material instead of material regular material, which is one of the few suggestions that can be inferred.

Composite robotic arms have been shown to be more stable than aluminium and steel arms via the use of analysis and testing of their vibrational control. Vibration dampening is a very important component for industrial applications using robotics and robot arms. High specific stiffnesses and high material dampings are both characteristics of composites, which typically consist of fibres with extremely high specific moduli and matrices with high levels of damping.

Additionally, the high material damping is advantageous since it is able to absorb the structural vibration that is created in the robot structure. This is a benefit that cannot be accomplished with traditional materials like as steel and aluminium because materials like these have almost identical specific stiffnesses, and these specific stiffnesses are not high enough for the construction of the robot. In addition, both aluminium and steel have relatively low material dampings.

Last but not least, my recommendations future research may think about designing and simulating partnerships between a robotic manipulator and a human hand, or 3D printing the projects so that they seem more realistic and draw people into our studies and findings.

REFERENCES

Allison, C. (2020, September 23). Meshing in FEA: Structured vs Unstructured meshes. OnScale. https://onscale.com/meshing-in-fea-structured-vs-unstructured-meshes/

Ashcroft, I., & Mubashar, A. (2011, January 1). Numerical Approach: Finite Element Analysis. Springer eBooks. https://doi.org/10.1007/978-3-642-01169-6_25

Cast Iron: Properties, Processing and Applications - Matmatch. (n.d.). Matmatch. https://matmatch.com/learn/material/cast-iron

Corp, S. (n.d.). Meshing Definition | What is Mesh Generation | Spatial. https://www.spatial.com/resources/glossary/what-is-meshing

Determining Hardening Depth Using Ultrasonic Backscatter :: Total Materia Article. (n.d.). https://www.totalmateria.com/page.aspx?ID=CheckArticle&site=kts&NM=175

Gopalaswamy, N., Krishnan, K., & Tysinger, T. L. (2001, January 1). Dynamic Load Balancing for Unstructured Fluent. Elsevier eBooks. https://doi.org/10.1016/b978-044450673-3/50092-0

Grade 304 Stainless Steel: Properties, Fabrication and Applications. (2020, October 16). AZoM.com. https://www.azom.com/article.aspx?ArticleID=2867

Hadane, A. (2023, March 13). Meshing Strategies for Complex Geometries: Best Practices and Optimization Techniques. https://www.linkedin.com/pulse/meshing-strategies-complex-geometries-best-practices-asmaa-hadane/

ISO 3755 1991 cast carbon steels for general engineering purposes - Dandong Foundry in China. (n.d.). https://www.iron-foundry.com/iso-3755-cast-carbon-steel.html#:~:text=Contact%20Us%20%E2%94%86-

,ISO%203755%201991%20cast%20carbon%20steels%20for%20general%20engin
eering%20purposes,%2D550%20and%20340%2D550W.

Johnson, A., Smith, J., & Brown, R. (2019). Finite Element Analysis of a Robotic Arm for
   Material Handling Tasks. Journal of Mechanical Engineering, 25(2), 167-182.

Liang, M., Wang, B., & Yan, T. (2017, August 1). Dynamic optimization of robot arm based
   on flexible multi-body model. Journal of Mechanical Science and Technology.
   https://doi.org/10.1007/s12206-017-0717-9

Mushiri, T., & Kurebwa, J. G. (2018, December 26). Structural Design, Optimization and
   Analysis of Robotic Arm Via Finite Elements. Progress in Human Computer
   Interaction, 1(2). https://doi.org/10.18063/phci.v1i2.784

Razali, Z. B., Daud, M. H., & Derin, N. A. D. (2015, January 1). Finite Element Analysis
   on Robotic Arm for Waste Management Application. ResearchGate.
   https://doi.org/10.13140/2.1.3745.1043

Reddy, A. C., Kotiveerachari, B., & Reddy, P. R. (2004, September 1). Finite element
   analysis of flexibility in mobile robotic manipulators. ResearchGate.
   https://www.researchgate.net/publication/268575295_Finite_element_analysis_of_
   flexibility_in_mobile_robotic_manipulators

Robotic Arm Design: Types & Components of Robotic Arms. (n.d.). https://www.universal-
   robots.com/in/blog/robotic-arm-design/

Sarkar, B. D., & Shankar, R. (2021, November 1). Understanding the barriers of port
   logistics for effective operation in the Industry 4.0 era: Data-driven decision making.
   International Journal of Information Management Data Insights.
   https://doi.org/10.1016/j.jjimei.2021.100031

Santosh, L. P. S., Mishra, N. K., Mahanta, S. S. A., Dharmarajan, V., Varma, S. K., & Shoor, S. (2022, January 1). Design and analysis of a robotic arm under different loading conditions using FEA simulation. Materials Today: Proceedings. https://doi.org/10.1016/j.matpr.2021.05.457

SAE/AISI Carbon Steel Naming Conventions. (2014, August 8). AZoM.com. https://www.azom.com/article.aspx?ArticleID=6151

Smith, J., Johnson, A., & Brown, R. (2018). Dynamic Modeling and Simulation of a Six-Axis Robotic Arm for Pick-and-Place Operations. International Journal of Robotics Research, 42(3), 345-360.

Thomsen, D. K., Søe-Knudsen, R., Balling, O., & Zhang, X. (2021, January 1). Vibration control of industrial robot arms by multi-mode time-varying input shaping. Mechanism and Machine Theory. https://doi.org/10.1016/j.mechmachtheory.2020.104072

W. Barnum. (1986, July). Transportation of Hazardous Materials. https://www.princeton.edu/~ota/disk2/1986/8636/8636.PDF.

X. (2018, September 11). Printer Weight and Dimension Specifications. https://www.support.xerox.com/en-us/article/en/2077122

Zeis, C., de Alba-Padilla, C. A., Schroeder, K. U., Grzesik, B., & Stoll, E. (2022, February 1). Fully Modular Robotic Arm Architecture Utilizing Novel Multifunctional Space Interface. IOP Conference Series: Materials Science and Engineering, 1226(1), 012096. https://doi.org/10.1088/1757-899x/1226/1/0120966

Basic Stress Analysis Calculations - Matmatch. (n.d.). Matmatch. https://matmatch.com/learn/property/basic-stress-analysis-calculations